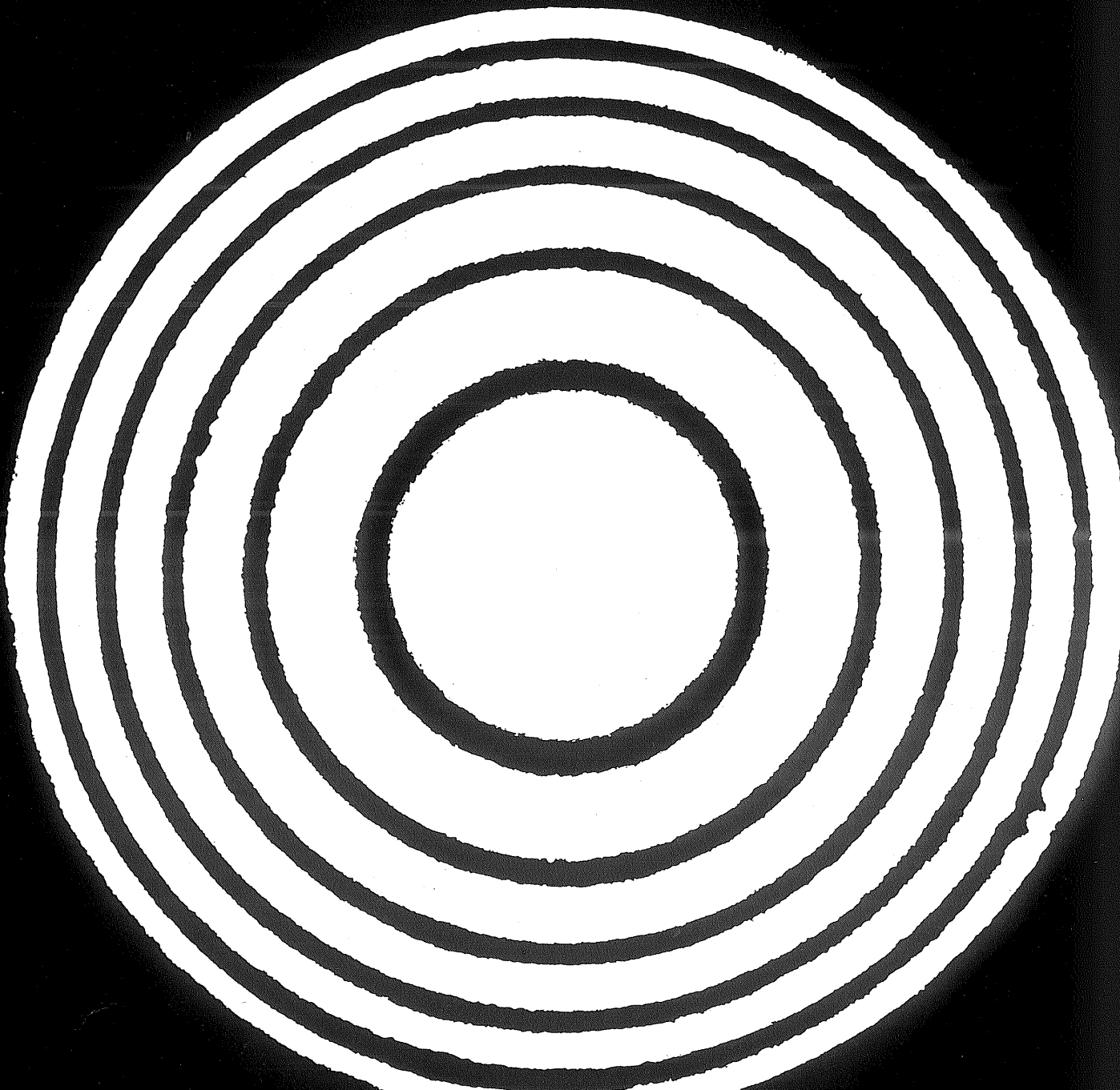


Interferogram Interpretation and Evaluation Handbook



Fourth Edition, April 1993
Third Edition, May 1984
Second Edition, December 1980
First Edition, October 1977

Copyright © 1977, by Zygo Corporation

Permission to reprint portions of this handbook
will be granted readily in most cases.
Please submit requests in writing.

Foreword

In addition to providing sophisticated interferometers and data reduction products, it has always been Zygo's desire to provide our customers (and other interferometer users as well) with a better understanding of the data reduction principles and techniques used to extract information from interference patterns. Zygo first published the Interferogram Interpretation and Evaluation Handbook in 1977 in response to the perceived need that developed from the popularity of Zygo's first interferometer product, the GH Interferometer. The Handbook explained how various interferometer systems were configured, and taught the basic techniques required to interpret interferograms. Even though computers and elaborate software programs are now used to analyze interference data, understanding the manual techniques provides an important background.

It is gratifying that, so many years after it was first published, Zygo has continued to receive requests for copies of the Handbook. Since copies of the 1984 third edition were no longer available, Zygo decided to reprint the Handbook again. This 1993 fourth edition is essentially identical to the previous editions, with the addition of the Foreword and Epilogue.

For those reading this Handbook who are Zygo customers, we thank you for your patronage and loyalty over these many years. It has been a pleasure serving you, and we will continue to strive to serve you with innovative, useful products of value in the future. For those of you who are not yet Zygo customers, we hope this Handbook will enhance your understanding, enjoyment, and use of interferometry, and that Zygo will have the opportunity to serve you in the future.

Contents

Section	Page
1 Introduction	2
2 Interferometry	3
3 Interpretation of Interferograms	4
3.1 General	4
3.2 Illustrative Examples	6
3.3 Phase Information	7
4 Evaluation of Interferograms	10
4.1 Manual Techniques	10
4.1.1 Mechanical Parallelogram: Technique #1	10
4.1.2 Mechanical Parallelogram: Technique #2	11
4.1.3 Electronic Parallelogram:	13
4.1.4 Other Manual Techniques	13
4.2 Sophisticated Techniques	13
4.2.1 Automatic Pattern Processor	13
4.2.2 Phase Measuring Interferometer	15
4.3 Relevance of Measurements	15
5 Glossary of Terms	16
6 References	17
Acknowledgments	17
Appendix A Interferograms Representing Individual and Combinations of Classical Aberrations	18
Appendix B Sample Interferograms with Evaluation Results	23

1 Introduction

This application bulletin is a practical handbook to aid in the interpretation and evaluation of interferograms. This bulletin contains the methodology needed to interpret interferograms, a glossary of terms, a comprehensive set of illustrative interferograms, and a reference reading list. Because interferometry is based on interfering wavefronts, this handbook emphasizes the concept of wavefronts.

The handbook has been written to be useful to readers with various levels of technical expertise and with different requirements. Therefore, a reader may, in general, find only portions of the handbook relevant.

Interferometric testing has long been used in optical metrology. The advent of the laser has not only made interferometry more convenient to use but has also extended its range of application. Interferometry is used as a tool in optical fabrication, final testing, and system alignment.^{1, 2, 3}

For most interferometry the output of the test is an interference fringe pattern which can be observed in real time and photographed to produce an interferogram. The type of pattern is determined by the particular measurement configuration and by the errors in the article under test. The quantitative reduction of an interference fringe pattern is usually based on ascertaining the fractional deviation of the interference fringe pattern from some ideal, best-fitting pattern. The denominator of the fractional deviation is the measured spacing between a pair of fringes in the ideal pattern.

The quantitative usefulness of an interference pattern is dependent upon having a method of data extraction and reduction. Interference pattern reduction can range in complexity from a simple visual evaluation to an elaborate reduction of the data extracted by an automatic microdensitometer with a large computer.⁴ In between these extremes there are a great variety of means for hand reduction.

2 Interferometry

An optical interferometer is a measuring instrument which utilizes the interference phenomenon based on the wave properties of light. Interferometers function by dividing a wavefront into two or more parts, principally a reference wavefront and a measurement wavefront, which travel different paths and which then recombine to form an interference fringe pattern. The geometrical properties of the interference fringe pattern are determined by the difference in optical path traveled by the recombined wavefronts. Interferometers measure the difference in optical paths in units of the wavelength, λ , of the light used. Since the optical path is the product of the geometrical path and the refractive index, an interferometer measures either the difference in geometrical path when the beams traverse the same medium or the difference of the refractive index when the geometrical paths are equal.

An important feature of an interference fringe pattern is the interferogram scale factor, i.e., whether one fringe spacing corresponds to $\lambda/2, \lambda$, or some other multiple of λ . The interferogram scale factor depends on the particular interferometric configuration and test setup. For example, when evaluating the single-pass wavefront distortion of a window in either a Twyman-Green or Fizeau interferometer (see Figure 2-1), the interferogram scale factor is one fringe corresponds to $\lambda/2$. However, if the window is evaluated in a Mach-Zehnder interferometer (see Figure 2-2), the interferogram scale factor is one fringe corresponds to 1λ .

Since it is not the purpose of this bulletin to provide a detailed discussion of either interferometers or interferometry, the reader is referred to References 5 through 13 for information on these subjects.

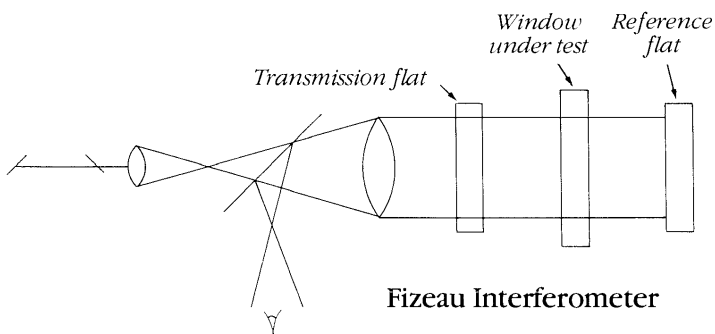


Figure 2-1(a)

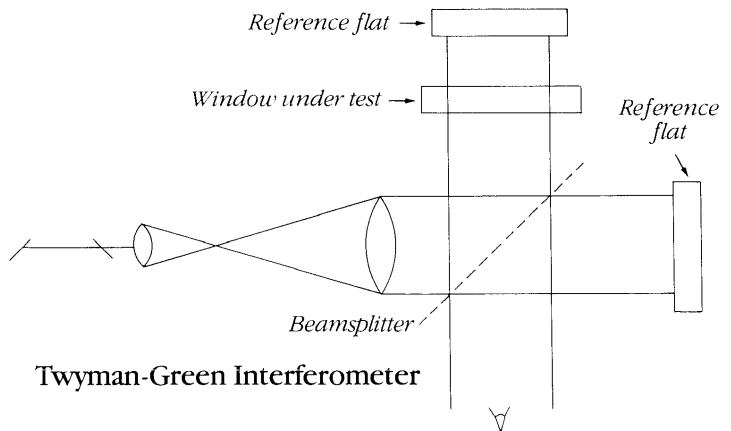


Figure 2-1(b)

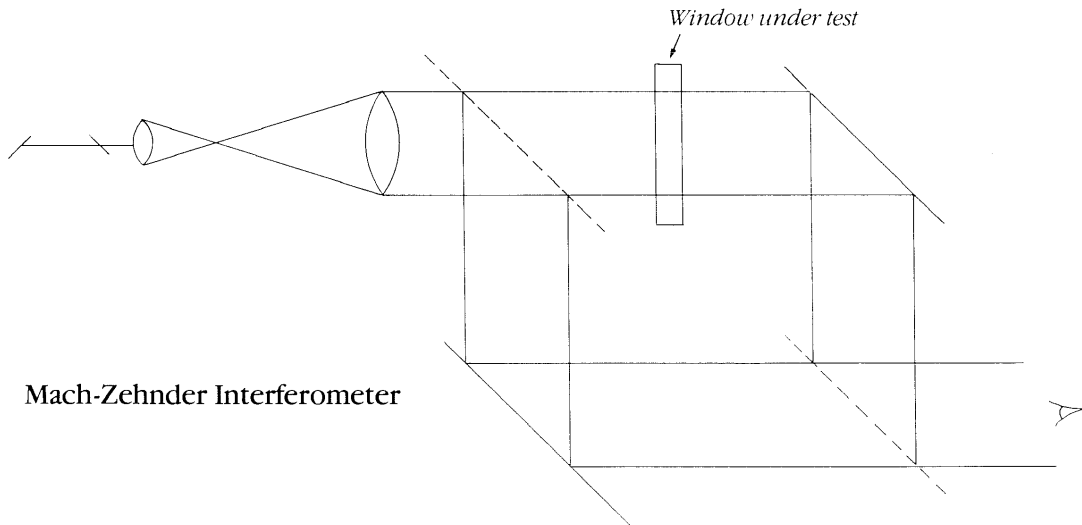


Figure 2-2

3 Interpretation of Interferograms

3.1 General

In order to interpret an interferogram, it is first necessary to know the interferogram scale factor, i.e., the quantitative relation defining the correspondence between a fringe spacing on the interferogram and the parameter of interest. The interferogram scale factor is determined by the fact that the space between fringes of like nature corresponds to an optical path difference of one wavelength between the measurement and reference wavefronts and by knowing the type of interferometric setup.

The commonly used interferometric setups can be categorized into one of two types; either the single-pass type or the double-pass type. In a single-pass type interferometer, the measurement beam traverses the item under test only once. In a double-pass type interferometer, the measurement beam traverses the item under test once and is then reflected back through the item under test a second time usually by an

auxiliary reflector. The measurement beam thusly traverses the item under test twice.

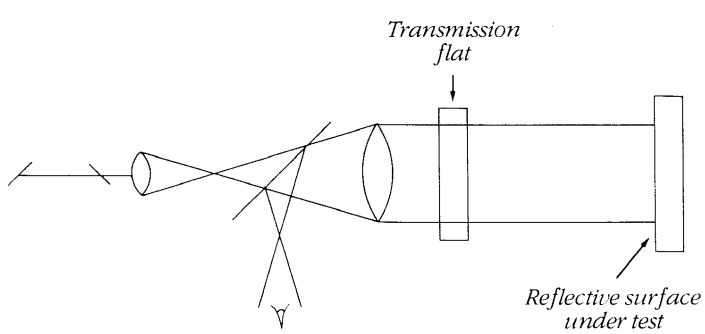
Therefore, for a single-pass transmitted wavefront measurement, e.g. the Mach-Zehnder, the interferogram scale factor is: one fringe spacing = λ , where λ is the wavelength used in the interferometer. However, when a reflecting surface, such as a plano mirror, is being evaluated at normal incidence the interferogram scale factor is: one fringe spacing = $\lambda/2$. The reason for this is that at normal incidence the reflected wavefront will have *twice* the error of the reflecting surface. Thus, when evaluating mirror surfaces at normal incidence, one fringe corresponds to one-half wavelength. Table 1 below lists the interferogram scale factor for some common interferometric setups and for a variety of measured parameters.

In the case of a retroreflector or cube corner, the quanti-

Table 1

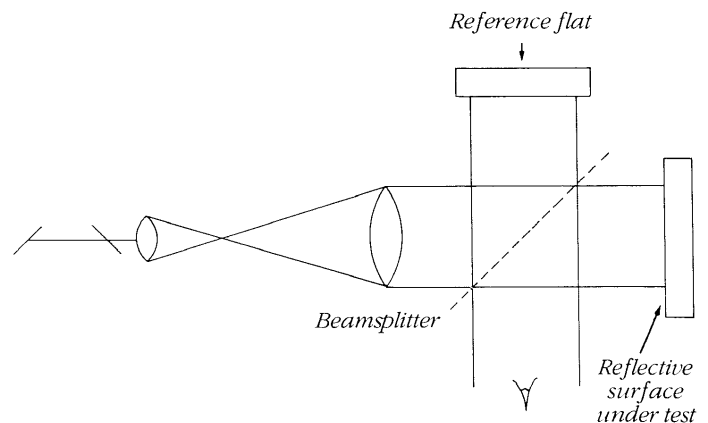
Interferogram Scale Factors for some Common Interferometric Setups
and for a Variety of Measured Parameters

Measured Parameter	Interferometric Setup	Interferogram Scale Factor	Typical Example
Reflective Surface	Normal Incidence, single pass	1 fringe spacing = $\lambda/2$	Figure 3.1-1
Reflective Surface	Angle of incidence = θ , single pass	1 fringe spacing = $\lambda/(2\cos\theta)$	Figure 3.1-2
Reflective Surface	Normal Incidence, double pass	1 fringe spacing = $\lambda/4$	Figure 3.1-3
Reflective Surface	Angle of incidence = θ , double pass	1 fringe spacing = $\lambda/(4\cos\theta)$	Figure 3.1-4
Single-pass Transmitted Wavefront Distortion	Single pass	1 fringe spacing = 1λ	Figure 2-2
Single-pass Transmitted Wavefront Distortion	Double pass	1 fringe spacing = $\lambda/2$	Figure 2-1
Double-pass Transmitted Wavefront Distortion	Single pass	1 fringe spacing = 2λ	Figure 2-2
Double-pass Transmitted Wavefront Distortion	Double pass	1 fringe spacing = 1λ	Figure 2-1



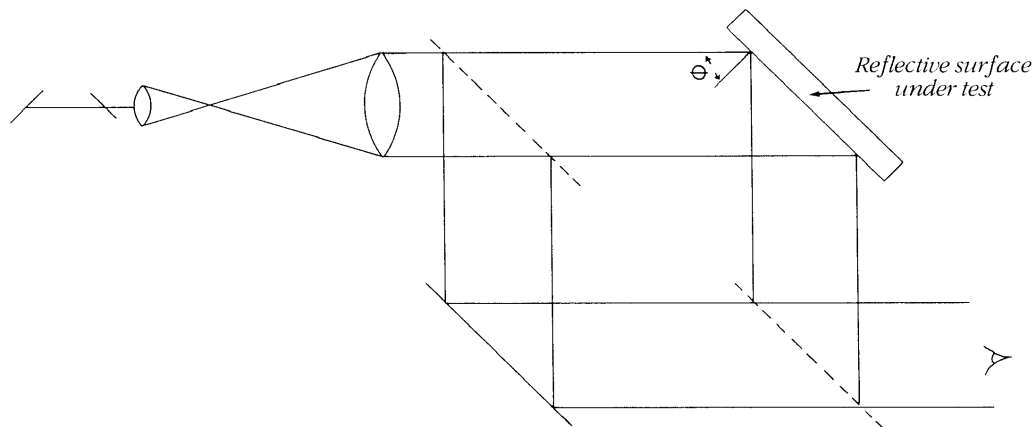
Fizeau Interferometer

Figure 3.1-1(a)



Twyman-Green Interferometer

Figure 3.1-1(b)



Mach-Zehnder Interferometer

Figure 3.1-2

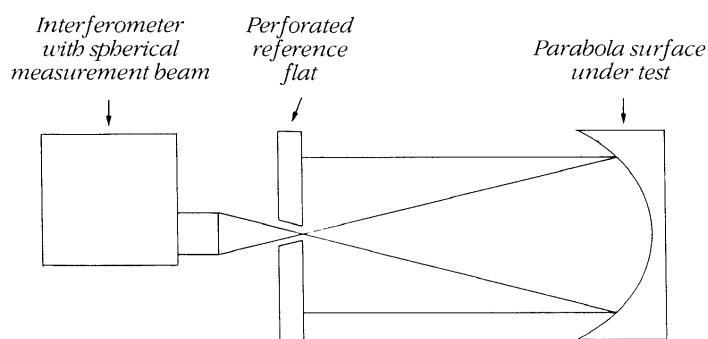


Figure 3.1-3

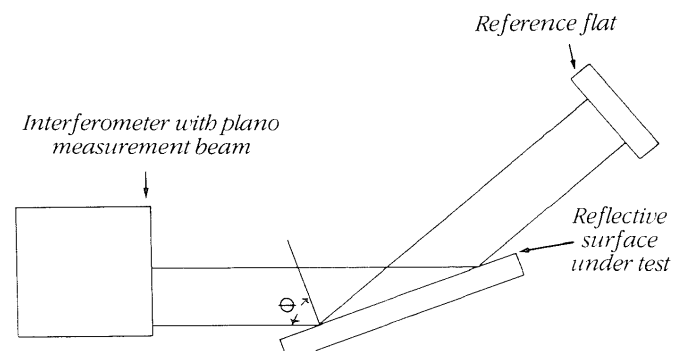
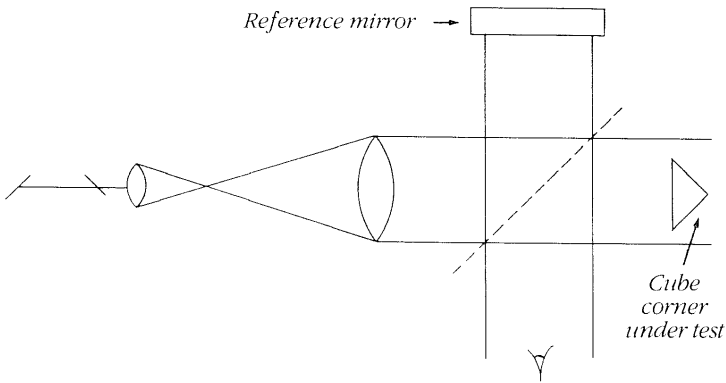


Figure 3.1-4

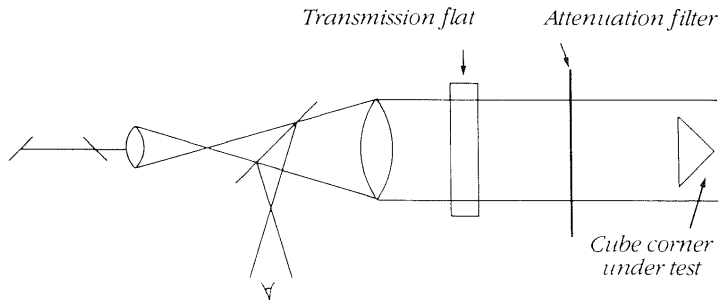
tative information with respect to wavefront distortion and angular deviation is contained in the output wavefront. This information can be extracted by comparing the output wavefront to a plane reference wavefront in either a Twyman-Green or modified Fizeau interferometer, see Figure 3.1-5. In this case, the interferogram scale factor is such that one fringe corresponds to one wavelength, since it is the wavefront and not the surface that is of interest.

Since a retroreflector acts like a mirror, and since mirror flatness is commonly evaluated using the one fringe corresponds to one-half wavelength interferogram scale factor, it is not uncommon to find retroreflectors which have been incorrectly evaluated because of the use of the incorrect interferogram scale factor.



Twyman-Green Interferometer

Figure 3.1-5(a)



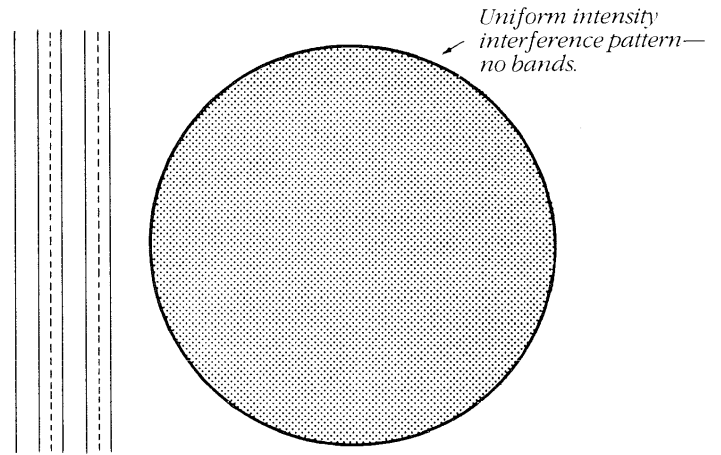
Modified Fizeau Interferometer

Figure 3.1-5(b)

3.2 Illustrative Examples

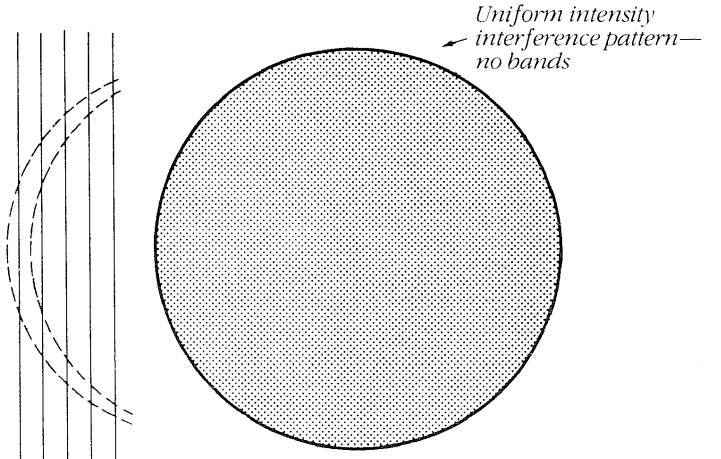
When two wavefronts of identical shape are perfectly superimposed, uniphase interference, also commonly referred to as a fluffed-out fringe, will result. See Figure 3.2-1. It is difficult to extract visually quantitative information from the fluffed-out fringe. Nevertheless, quantitative information can be extracted from the fluffed-out fringe using photoelectric techniques. For example, distance measuring interferometers are based on photoelectric sensing of the fluffed-out fringe. In addition, very flat Fizeau interferometer surfaces are sometimes evaluated by a photoelectric evaluation of the fluffed-out fringe.

If a slight tilt is introduced between the two wavefronts, the resulting fringe pattern will be a family of parallel,



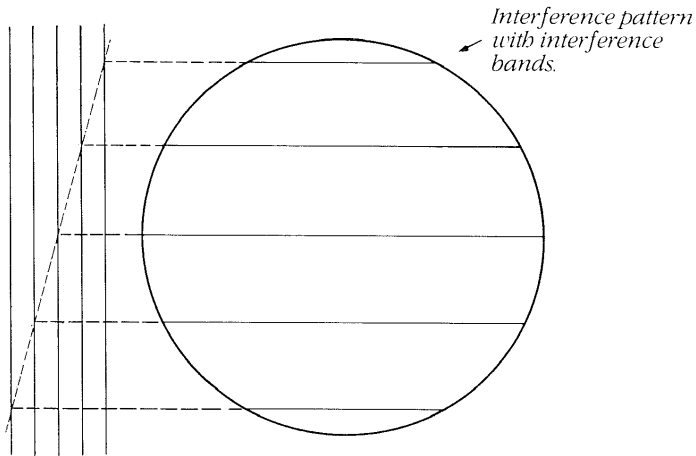
Interference of plano wavefronts — no relative tilt.

Figure 3.2-1(a)



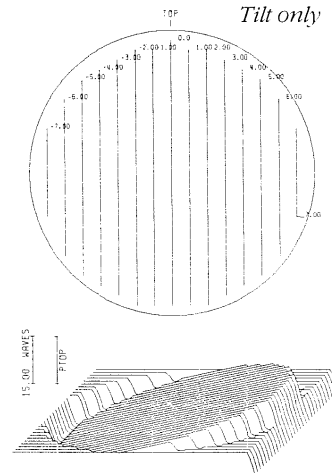
Interference of two spherical wavefronts with same radius of curvature and no relative tilt.

Figure 3.2-1(b)



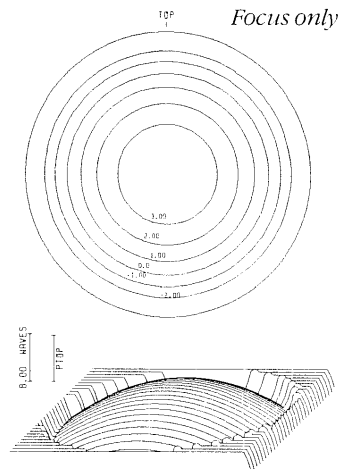
Interference of plane wavefronts with relative tilt.

Figure 3.2-2



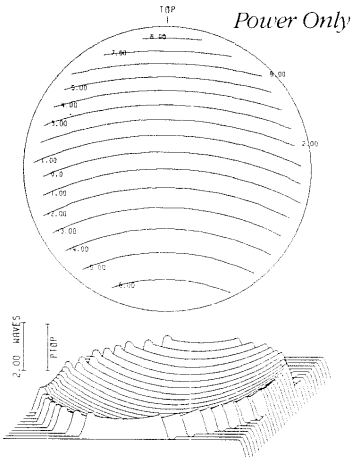
Perfect Test Wavefront

Figure 3.2-3(a)



Perfect Test Wavefront

Figure 3.2-3(b)



Interference with slight tilt and power shift.

Figure 3.2-4

3.3 Phase Information

A static interference pattern or interferogram alone contains no phase information, i.e., whether the distortion is a peak or a valley. Since it is important not only when attempting to fabricate an optical element or surface but also when assembling optical systems to know whether the distortion corresponds to a peak or a valley, the extraction of phase information is important. In order to ascertain phase information, it is necessary to ascertain and record the location of the zero order of the interference pattern. The zero order is located where there is zero optical path difference between the interfering wavefronts. In order to locate the zero order, one can alter the interferometer cavity in a known way and note the direction of the motion of the fringes. Referring to

Figure 3.3-1(a), if the interferometer cavity spacing is decreased as shown, the fringes move away from the direction of the zero order. Conversely, if the interferometer cavity spacing is increased, the fringes move toward the zero order, Figure 3.3-1(b).

Similarly, one can locate the zero order for nominally plane wavefronts by altering the tilt of the interferometer cavity or interfering wavefronts in a known direction and by noting the direction of motion of the fringes. Referring to Figure 3.3-2, if the tilt is decreased as shown, the fringes move away from the direction of the zero order. Conversely, if the tilt is increased, the fringes move toward the zero order. Figure 3.3-3 illustrates the physical basis for this behavior.

In practice, it may not be possible to alter only one of the geometrical parameters of the interferometer cavity. When done manually, usually both spacing and tilt of the cavity change, e.g. when one pushes on one element of the interferometer cavity, not only will the cavity spacing decrease but the tilt will, in general, also change in some unknown fashion about some unknown pivot point. Therefore, to ascertain unambiguously the direction of the zero order, it is necessary to observe and note 1) the change in fringe spacing and 2) the overall surface or wavefront geometry represented in the interference pattern in addition to the direction or directions of fringe motion.

Fringe spacing is a measure of tilt. See Figure 3.3-3. Therefore, changes in fringe spacing convey changes in tilt when the interferometer cavity geometry is altered. An increase in fringe spacing indicates a decrease in tilt, and a decrease in fringe spacing indicates an increase in tilt.

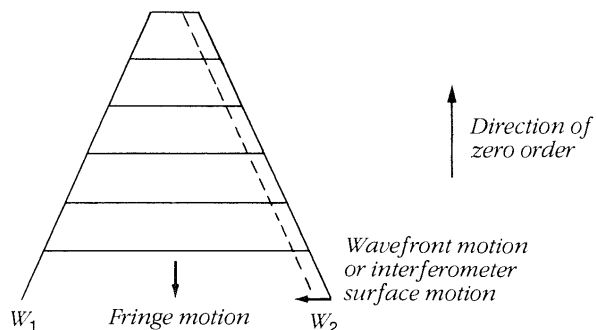


Figure 3.3-1(a)

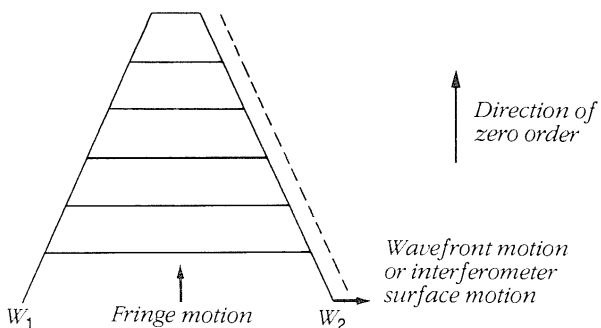


Figure 3.3-1(b)

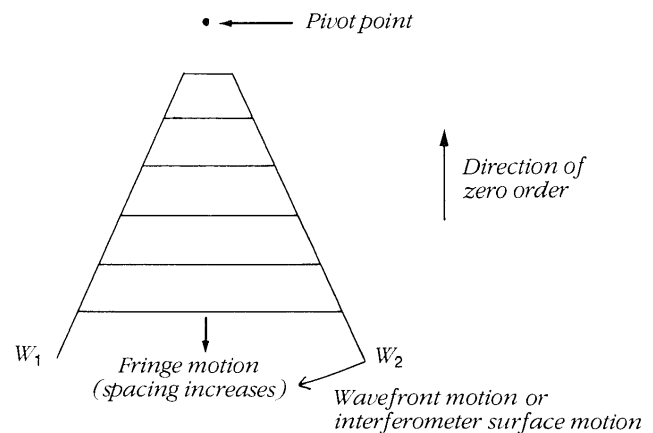


Figure 3.3-2

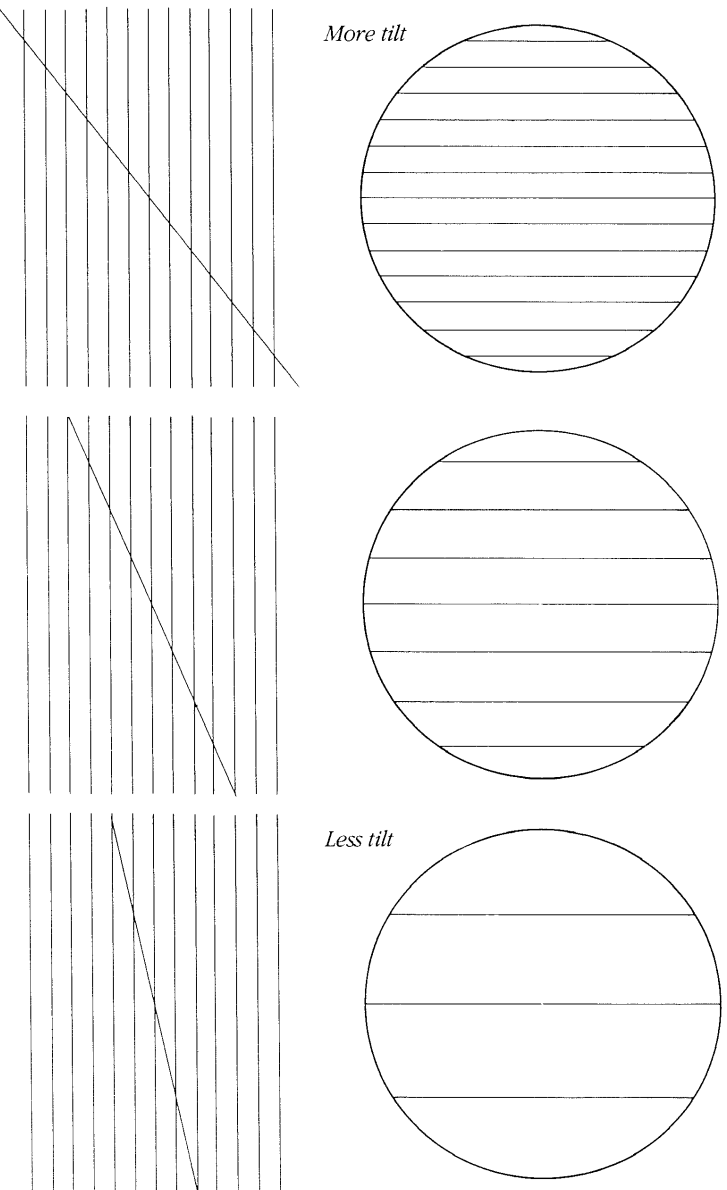


Figure 3.3-3

It should be noted that the zero order may be located in more than a single direction. For example, with a concave cylindrical surface evaluated with zero tilt, the zero order is located in two directions, i.e., on opposite sides of the cylinder axis.

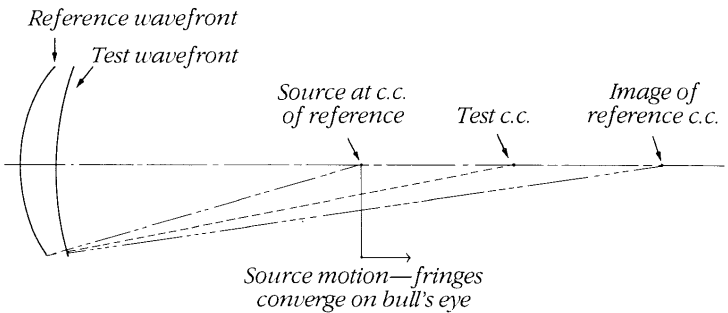
With a centered circular interference pattern, the fringes are formed by the path difference between two spherical wavefronts whose centers of curvature do not coincide. Coincidence implies the "fluffed" out fringe condition described earlier. Consider one spherical wavefront to be the reference and the other the test wavefront. If the radius of the test wavefront is longer than the radius of the reference, the test wavefront will be convex to the reference (see Figure 3.3-4). When the radius of the test wavefront is shorter than that of the reference wavefront, the test wavefront will be concave to the reference (see Figure 3.3-5). If an adjustment is made to obtain coincidence of the two centers of curvature, the fringes in each case will appear to converge on the bull's-eye fringe. When the test wavefront is convex to the reference, the fringes curve toward the zero order and for the concave case away from it.

For the general case where the fringes are neither circular nor straight, a combination of these facts apply. First determine the direction of the zero order as described for straight fringes. Second, observe the direction the fringes curve relative to the zero order to determine whether the surface is convex or concave. This same rule applies for local distortions as well.

Figures 3.3-6 and 3.3-7 illustrate the technique commonly used to ascertain the nature of a spherical surface.

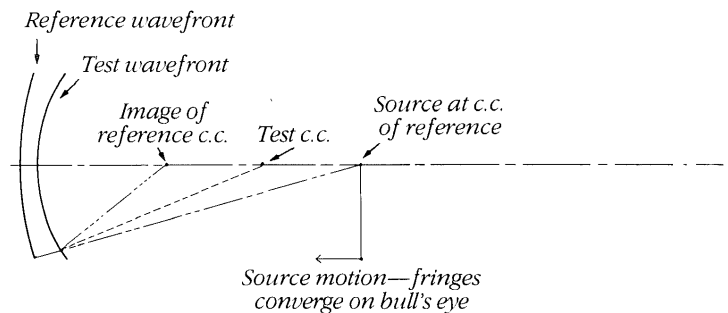
There may be cases where the above definitions of zero order do not strictly apply over the entire area of the interference pattern. For example, a fringe pattern consisting of a large number of local, enclosed fringes suggests a part with many localized hills and valleys. Determination of the phase of these distortions requires the examination of each one relative to the surrounding pattern using the appropriate definition for zero order. Simple tilt adjustments will cause the fringes to move in varying directions depending on the local error so that each one needs to be defined on the basis of the fringe motion nearest it.

Observing zero order whether it is local or global requires a dynamic adjustment. One must not lose sight of the fact that this adjustment which changes the spacing also changes the air wedge between the two surfaces under test. A change in spacing without a change in air wedge is virtually impossible to achieve. It is necessary in some cases to ascertain not only the direction in which the fringes are moving but also their relative spacing since both changes may occur. Generally the simple wedge change for the cases described above will be the dominant change and the observed fringe pattern motion will follow the rules given. The above statements are given as a caution to those who may be testing highly unusual surfaces, and in those instances additional observations may be necessary when the dynamic adjustments are made.



Reference center of curvature (c.c.) inside focus

Figure 3.3-4



Reference center of curvature (c.c.) outside focus

Figure 3.3-5

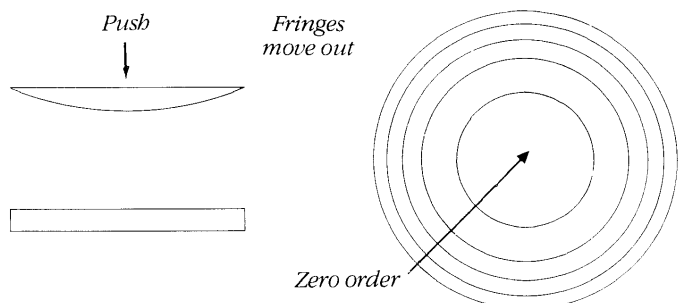


Figure 3.3-6

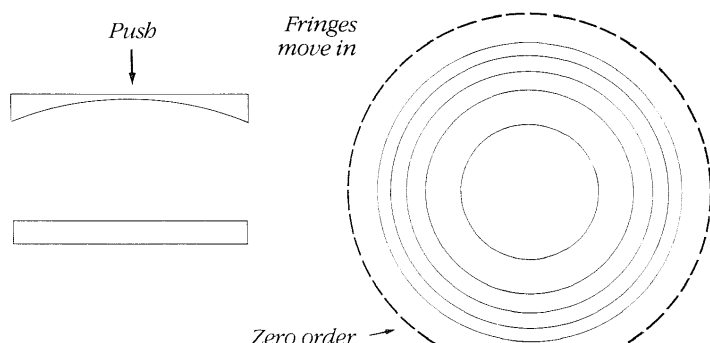


Figure 3.3-7

4 Evaluation Of Interferograms

In order to evaluate an interference fringe pattern, it is necessary to quantify the deviation of the fringe pattern from some ideal, best-fitting pattern. Optimally, the fit of the ideal pattern to the fringe pattern should be based on a least-squares computation. The deviation, denoted distortion, is usually presented as a fraction of the spacing between a pair of fringes in the ideal pattern, see Figure 4-1.

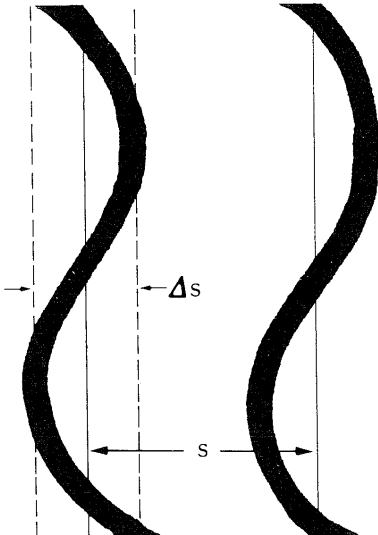


Figure 4-1

Quantitatively, $\Delta s/s$ is the fractional distortion in the fringe spacing, where s is the fringe spacing in the best-fitting pattern and Δs is the maximum deviation of the fringe pattern from the best-fitting pattern. The distortion in the parameter of interest in units of wavelengths is equal to the product of $(\Delta s/s)$ and the interferogram scale factor, i.e.,

$$(\Delta s/s) \cdot (\text{Interferogram Scale Factor}).$$

For example, when evaluating a mirror surface at normal incidence, using the test setup shown in Figure 3.1-1, the interferogram scale factor is one fringe = $\lambda/2$. Therefore, the surface distortion = $(\Delta s/s) \cdot (\lambda/2)$ in fractions of a wavelength.

In order to obtain the distortion at a wavelength different from that used in the interferogram, the following relation is used

$$(\text{Distortion})_{\lambda} = \frac{\lambda_{\text{INT}}}{\lambda} (\text{Distortion})_{\text{INT}}$$

Where $(\text{Distortion})_{\lambda}$ is the distortion in units of λ , λ_{INT} is the interferogram wavelength, λ is the wavelength different from λ_{INT} , and $(\text{Distortion})_{\text{INT}}$ is the distortion obtained from evaluating the interferogram.

For example, if $(\text{Distortion})_{\text{INT}} = \lambda/5$ where $\lambda_{\text{INT}} = 632.8 \text{ nm} = 0.633 \text{ micrometers}$ and $\lambda = 10.6 \text{ micrometers} = 10600 \text{ nm}$, then

$$(\text{Distortion})_{10.6} = \left(\frac{0.633}{10.6} \right) \left(\frac{1}{5} \right) = \frac{\lambda}{84}$$

where $\lambda = 10.6 \text{ micrometers}$.

4.1 Manual Techniques

For interference patterns with low to moderate distortion, i.e., $<1\lambda$, the techniques described in Sections 4.1.1 and 4.1.2 are useful. For interference patterns with large distortion, i.e., $>1\lambda$, the technique described on page 275 of Reference 7 is useful.

4.1.1 Mechanical Parallelogram: Technique #1

A common technique for reducing interferograms by hand is based on using a device comprised of a hinged mechanical parallelogram with a number of equally-spaced, hinged members to produce a grid of parallel, equally-spaced straight lines of variable spacing.

Figure 4.1-1 shows a hinged parallelogram device.

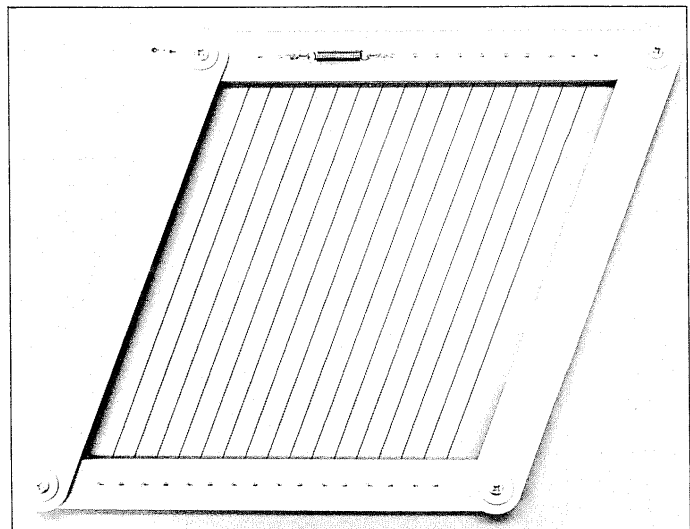


Figure 4.1-1

A procedure for evaluating an interferogram with this device is given below:

Step 1. Adjust the device so the grid lines are a best-fit to the fringe pattern—see Figure 4.1-2. Be sure the fit applies over the entire set of fringes and not to just the end fringes, for example. Operationally, the best “eye-ball” fit is achieved by simultaneously requiring 1) that the areas between the fringes and the grid lines lying on opposite sides of the grid lines are equal and 2) that each area is a minimum, i.e., made as small as possible. An error is introduced if the “eye-ball”

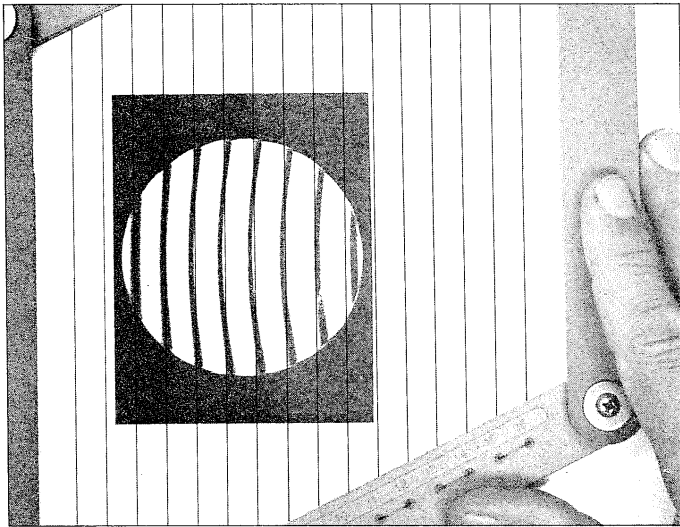


Figure 4.1-2

fit deviates from the optimal least-squares fit. Nevertheless, for many applications, an “eye-ball” fit is adequate, especially if an unbiased, global fit is used.

It is now necessary to measure the maximum deviation of a fringe from the best-fitting grid line corresponding to that fringe. Steps 2 through 5 outline the procedure to accomplish this measurement.

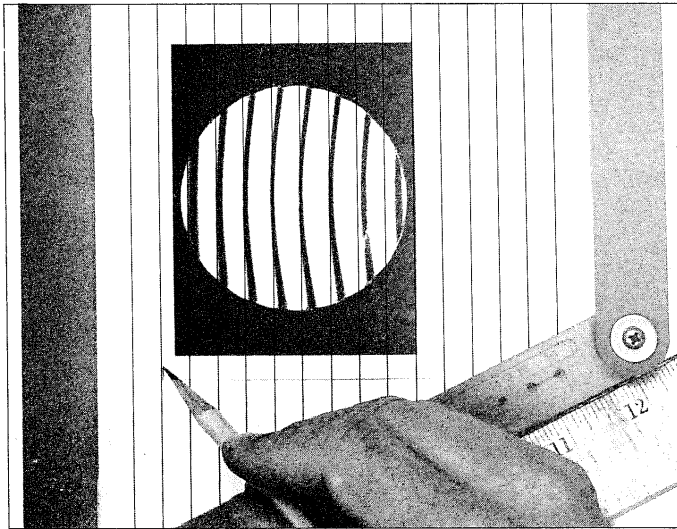


Figure 4.1-3

Step 2. Without rotating or changing the line spacing of the grid, move it to one side of the fringe pattern but such that a grid line still passes through the center of a portion of its corresponding fringe (see Figure 4.1-3). Mark this position on the interferogram.

Step 3. Move the grid, without rotating or changing the line spacing of the grid, to the other side of the fringe pattern but such that a grid line still passes through the center of a portion of its corresponding fringe (See Figure 4.1-4). Mark this position on the interferogram also.

Step 4. Measure the distance between the two marks made in Steps 2 and 3.

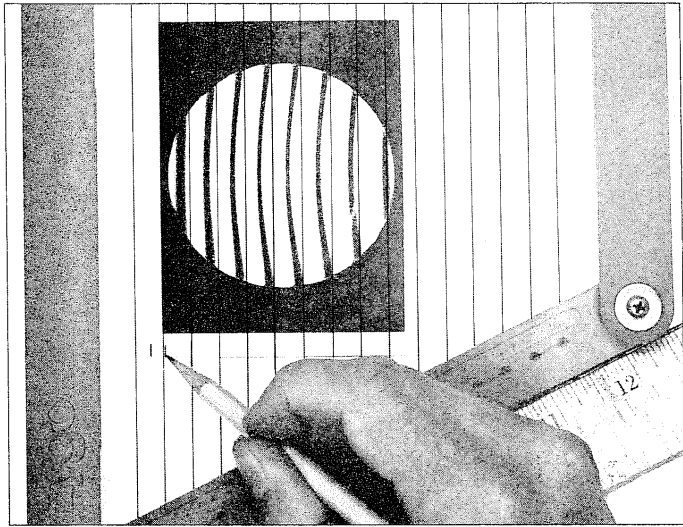


Figure 4.1-4

Step 5. Measure the distance between the two outermost lines on the grid and divide this distance by the number of fringe spaces to obtain the average spacing.

Step 6. Divide the measurement in Step 4 by the average spacing obtained in Step 5 to obtain the peak-to-valley fractional fringe distortion.

Step 7. Multiply the fractional fringe distortion by the interferogram scale factor to convert the fringe distortion to wavelengths.

4.1.2 Mechanical Parallelogram: Technique #2

Since the prescription for ascertaining the best-fitting grid suggested in Section 4.1.1 may not be sufficiently definitive for some applications, this section provides an alternative mechanical technique.

Step 1. Orient the interferogram so that the fringes are nominally vertical. Using a straightedge, draw two parallel lines (L_1 and L_2) which are perpendicular to the fringe pattern and which are spaced by 65% - 75% of the clear aperture diameter. See Figure 4.1-5.

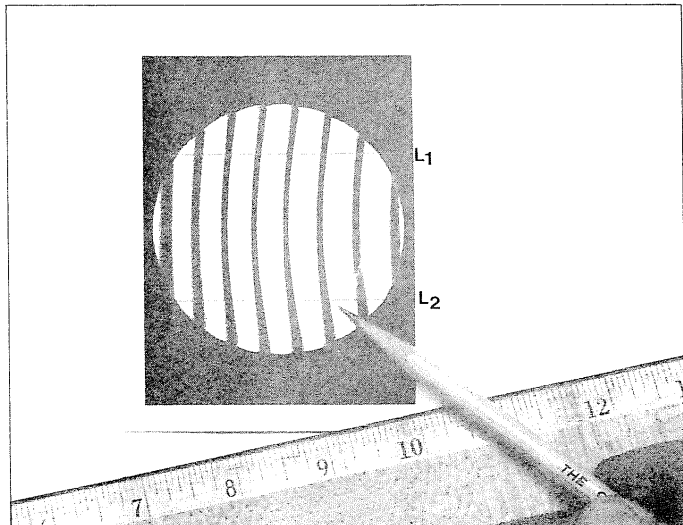


Figure 4.1-5

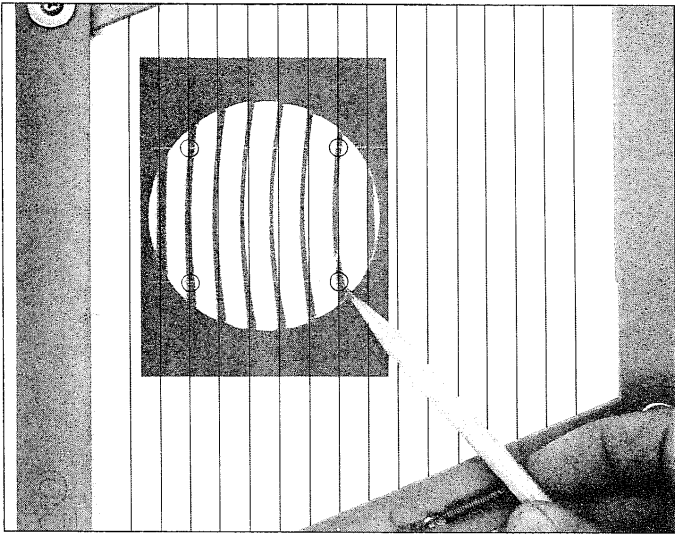


Figure 4.1-6

Step 2. Adjust the mechanical parallelogram so that the spacing between the left-most and right-most fringe and grid lines are identical. There should, of course, be the same number of grid lines and fringes. This adjustment is made trying to minimize the difference in spacing between the grid lines and the fringes in the circles shown in Figure 4.1-6. These circles are centered on the intersection of the two parallel lines L_1 and L_2 and the centers of the outermost fringes.

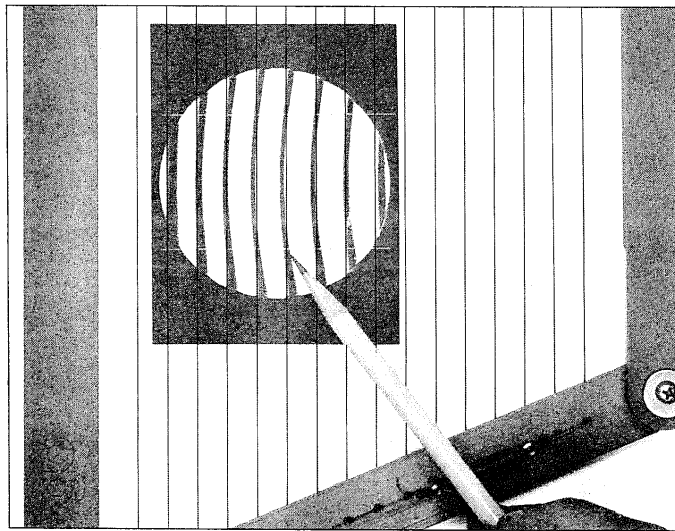


Figure 4.1-7

Step 3. Without changing the grid spacing, line up the grid line corresponding to the center fringe with the two points of intersection of the lines L_1 and L_2 and the center of the center fringe. See Figure 4.1-7.

It is now necessary to measure the maximum deviation of a fringe from the best-fitting grid line corresponding to that fringe. Steps 4 through 9 outline the procedure to accomplish this measurement. (This is the same procedure as Steps 2 through 7 in Technique # 1.)

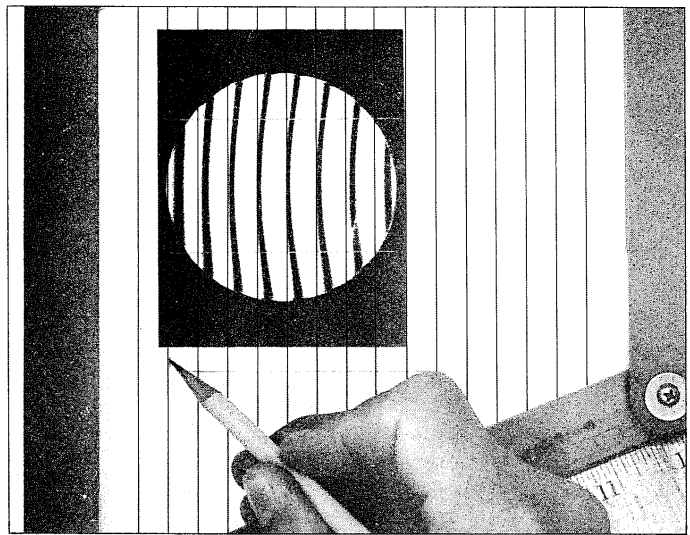


Figure 4.1-8

Step 4. Without rotating or changing the line spacing of the grid, move it to one side of the fringe pattern but such that a grid line still passes through the center of a portion of its corresponding fringe (see Figure 4.1-8). Mark this position on the interferogram.

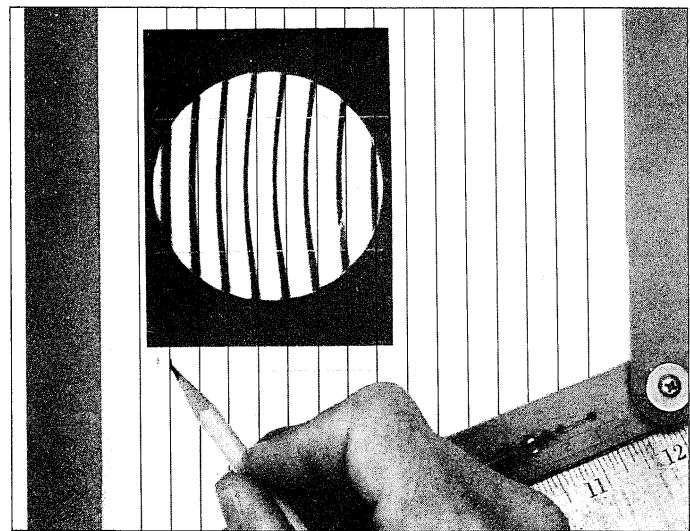


Figure 4.1-9

Step 5. Move the grid, without rotating or changing the line spacing of the grid, to the other side of the fringe pattern but such that a grid line still passes through the center of a portion of its corresponding fringe (See Figure 4.1-9). Mark this position on the interferogram also.

Step 6. Measure the distance between the two marks made in Steps 4 and 5.

Step 7. Measure the distance between the two outermost lines on the grid and divide this distance by the number of fringe spaces to obtain the average spacing.

Step 8. Divide the measurement in Step 6 by the average spacing obtained in Step 7 to obtain the peak-to-valley fractional fringe distortion.

Step 9. Multiply the fractional fringe distortion by the interferogram scale factor to convert the fringe distortion to wavelengths.

Appendix B contains a number of sample interferograms with numerical data based on a computer evaluation. These interferograms can be used for practice to establish confidence in evaluating interferograms.

4.1.3 Electronic Parallelogram

A few years ago Zygo introduced the novel electronic Zygo Interference Pattern Processor,* ZIPP, which is used with a CCTV. This electronic video parallelogram generator is a substantial improvement over the mechanical parallelogram or other manual techniques because 1) the three parameters, i.e., tilt, offset, and spacing, are independently adjustable, 2) it electronically measures the quantities of interest, and 3) it provides a digital display of the fractional peak-to-valley distortion. Figure 4.1-10 is a photograph of a CCTV monitor screen showing the fringe pattern, the electronically generated grid, and the digital read-out. ZIPP was designed to be used conveniently with a variety of manual techniques.

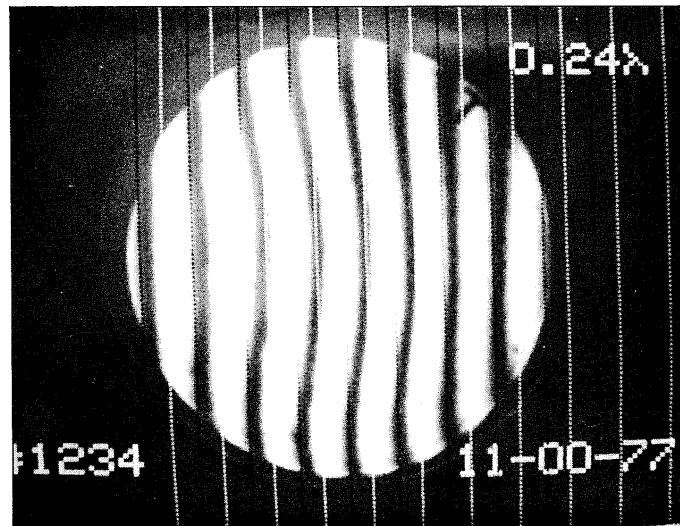


Figure 4.1-10

4.1.4 Other Manual Techniques

A great variety of manual techniques for evaluating interferograms have been published and are in use. Most of the techniques differ from the ones provided in 4.1.1 and 4.1.2 in the way in which the ideal pattern is determined. For example, one popular technique determines the ideal grid from two points located on the extremes of a fringe at one side of the pattern and a single point located on the center of a fringe at the other side of the pattern.

Since the ideal pattern must fit the fringe pattern optimally, in a least-squares sense, over the entire pattern, techniques which use an ideal pattern based on one or two fringes or only parts of fringes introduce a bias and an error whose magnitude is proportional to the distortion. For a perfect interference pattern, most manual techniques have the same quantitative level of systematic errors. When there is signifi-

cant distortion, techniques which do not use an ideal pattern based on an optimal fit, in a least-squares sense, will lead to distortion values larger than those from the optimal fit. Therefore, it behooves someone selling optical components or systems based on the reduction of interferograms to use a technique which is based on an optimal fit. From the point of view of someone purchasing optical components or systems based on the reduction of interferograms, a less than optimal fit simply assures him of a quality better than that derived from the measurement.

Besides techniques which can be categorized as less than optimal, a number of erroneous techniques are sometimes used. A common error is to obtain a distortion value based on the non-straightness of the fringes while ignoring the distortion in fringe spacing, or vice versa. Clearly erroneous techniques can lead to smaller distortion values than those from either the optimal or non-optimal techniques. Therefore, it is essential to understand the detailed procedure used to evaluate an interferogram before a confidence level can be assigned to the numbers provided.

4.2 Sophisticated Techniques

An increasing number of optical elements and systems require correction and evaluation to measurement accuracies of from $\lambda/50$ to $\lambda/100$. Hand measurement to these orders of accuracy with repeatability is very time consuming and frequently inadequate. To effectively carry out evaluations of $\lambda/50$ to $\lambda/100$ or to objectively certify optics to $\lambda/10$ or better requires an interferogram measuring system with $\lambda/50$ accuracy (approximately five times better).

The reduction of interferograms by hand is further complicated when there is a power or a focus error which produces a curvature in the fringes. The bull's-eye pattern with non-uniformly spaced concentric circles is a familiar example. Hand reduction of these complex fringe patterns is extremely tedious and time consuming. In order to extract the information from the interferogram, it is necessary to measure the two-dimensional coordinates for an array of points located on the center of the fringes and carry out a least-squares computation.

Sophisticated, expensive instruments have been designed and built for the high precision, automatic reduction of interferograms, see References 15 through 17. However, only a few facilities have access to these systems.

4.2.1 Automatic Pattern Processor

The availability of powerful microcomputers has made possible the design of sophisticated and affordable instrumentation to overcome the last major difficulty in the use of interferometry, the rapid, accurate and objective evaluation of the resultant interference pattern. Such interference pattern evaluation instrumentation is now commercially available to support the expanded use of interferometry.¹⁸

Zygo is currently marketing the Zygo Automatic Pattern Processor* (ZAPP) which has superseded the less advanced ZIPP parallelogram generator. ZAPP provides a sophisticated,

*U.S. Patent No. 4,141,038

*U.S. Patent Nos. 4,169,980 and 4,159,522.

automatic interference pattern evaluation capability. To evaluate either a real-time interference pattern or an interferogram with ZAPP, the operator simply pushes a button. ZAPP automatically acquires the fringe center coordinates, performs a complete least squares computation, and displays the fringe centers and calculated values on a video monitor. It takes ZAPP 1/60 second to acquire the two-dimensional (X,Y) coordinates of approximately 500 fringe centers. The least squares computation can be performed with or without power to provide the peak-to-valley distortion, the root-mean-square value of the distortion and the Optical Path Differences.

ZAPP was designed to be compatible with the Zyglo Mark II Interferometer or GH Mainframe modified with a suitable TV viewing system, or any other interferometer with a suitable TV viewing system. The standard ZAPP system includes an interferogram reader, processor module, control terminal, video monitor and video camera. An optional digital printer and/or an auxiliary computer can also be added to the system. The Zyglo FRINGE Program can be run on the computer to automatically provide a variety of optical computations.

The procedure for evaluating an interferogram and obtaining display outputs with ZAPP is given below. To perform each step of the procedure, the operator is only required to manipulate various automatic controls on the ZAPP control terminal. This sophisticated evaluation technique can be compared with the manual techniques described in Section 4.1.

Step 1. Insert input information, select operations, and select outputs using the prompting format provided by ZAPP.

Step 2. Define the clear aperture for testing by positioning the four cursors superposed over the fringe pattern on the video monitor. See Figure 4.2-1.

Step 3. Enter a request for ZAPP to automatically acquire the fringe centers (see Figure 4.2-2). Manual acquisition controls are also available for manually erasing and inserting fringe centers.

Step 4. Initiate the automatic least squares computation. Two results of the computation, the peak-to-valley (PV) and the root-mean-square (RMS) will appear on the video monitor in approximately three seconds. See Figure 4.2-3.

Step 5. Enter a request for ZAPP to store the optical path differences (OPDs) on a uniform grid in the microprocessor memory.

Step 6. Request an isometric view of the OPD data (see Figure 4.2-4) and the reciprocal of the data (see Figure 4.2-5).

ZAPP also provides separate operating modes which can automatically subtract power from an interferogram or perform accept/reject calculations according to specific tolerance limits entered by the operator. In addition, optional programs are available for measuring fringe patterns with obscurations and for calculating the maximum slope between adjacent fringe points.

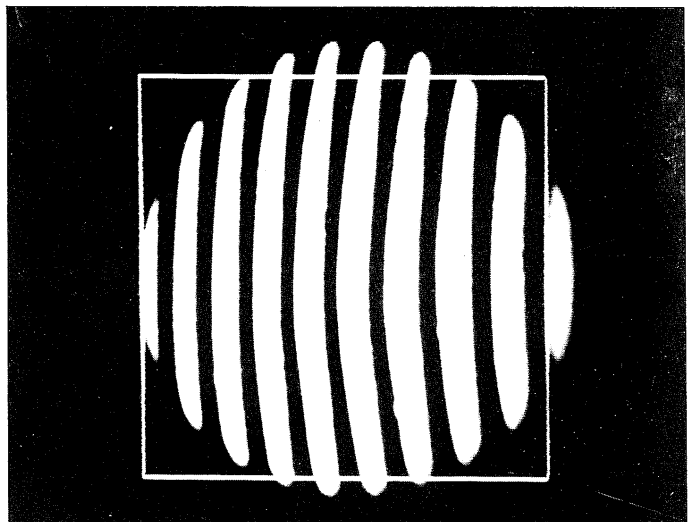


Figure 4.2-1

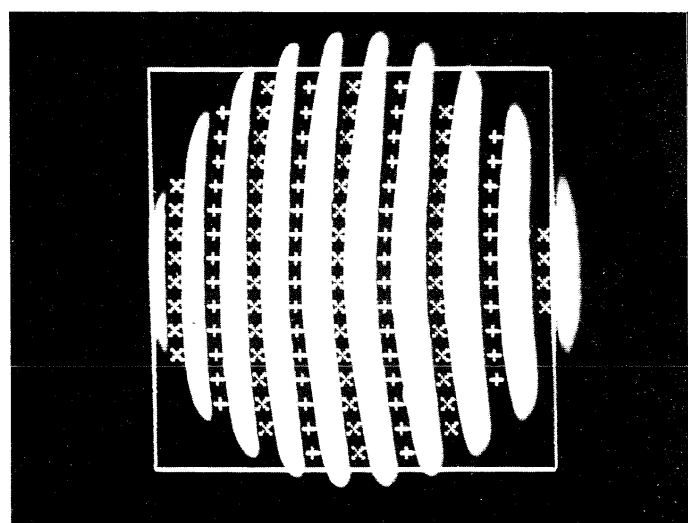


Figure 4.2-2

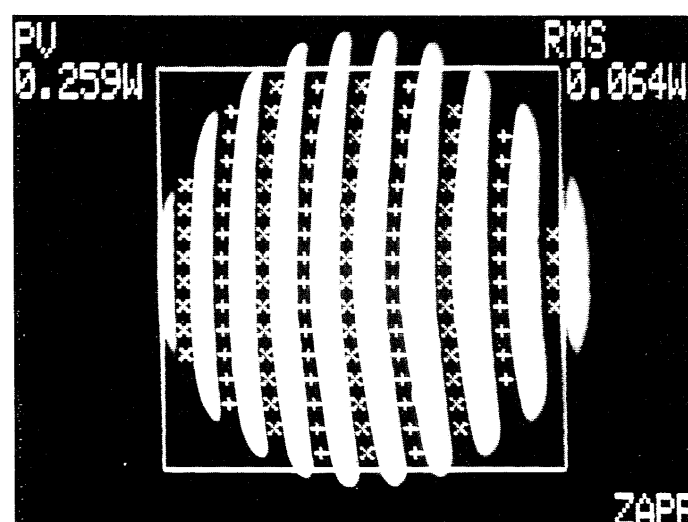


Figure 4.2-3

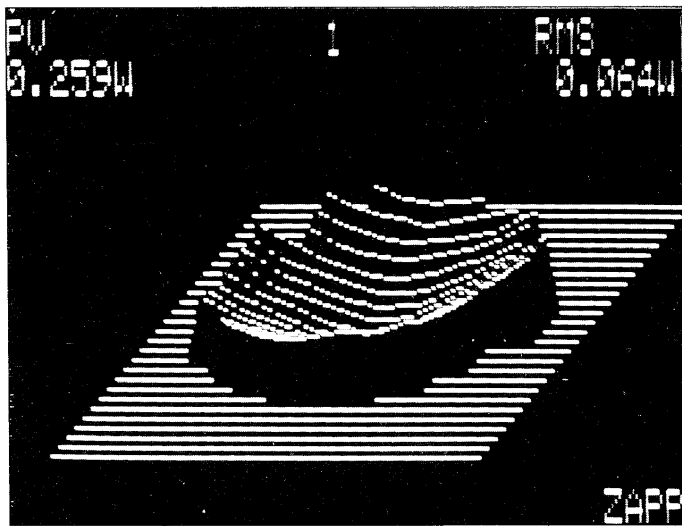


Figure 4.2-4

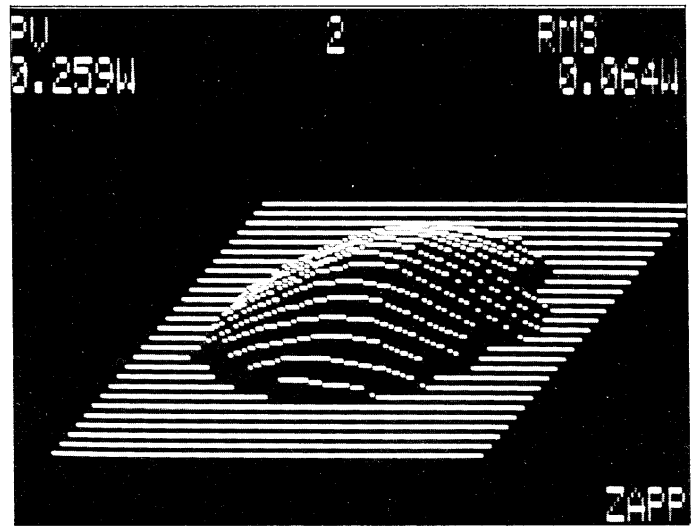


Figure 4.2-5

4.2.2 Phase Measuring Interferometry

Phase measuring interferometry is capable of providing high data density, and is insensitive to both the intensity profile of the beam and any geometrical distortion in the optics or detector to first order. This makes a phase measuring technique potentially more accurate than fringe pattern interferometry. It also enables the measurement of wavefronts of any fringe geometry and complexity as long as the maximum fringe density does not exceed one fringe/two pixels. Various methods have been developed to measure, in realtime, the phase difference between the two optical wavefronts of the interferometer. These methods fall into two categories: Stationary Phase Measurement and Dynamic Phase Measurement.

Stationary Phase Measurement. In stationary phase measurement, the phase between the two wavefronts of the interferometer is changed by a known amount and the light intensity is detected at each data point of the interference pattern. This is done repeatedly in three or more steps.^{16,20} During each step, the intensity data is stored and used later to compute the phase difference between the two wavefronts. Changing the phase is accomplished by increasing or reducing the optical path for the wavefront in one arm of the interferometer. Either a vidicon or diode array camera can be used as a detector since the only requirement is to detect intensities of stationary patterns.

Dynamic Phase Measurement. Dynamic phase measurement is also referred to in the technical literature as heterodyne interferometry.^{21,22} The phase of one wavefront is continuously changed, introducing a frequency difference between the two wavefronts. As a result the interference pattern is modulated continuously by the frequency difference. The light intensity of the interference pattern is then detected, while modulation occurs, to provide the phase data. A variety of methods have been developed to

modulate the interference pattern and detect the phase.

Dynamic phase measurement is superior to stationary phase measurement since data can be acquired at a higher rate thereby making the interferometer system less sensitive to mechanical vibrations and air turbulence.

The Zygo Mark III Interferometer System is a commercial interferometer which has dual data processing capabilities. It can evaluate real-time or (as an option) hard copy interference patterns using fringe pattern interferometry; and it can also perform phase interferometry. In the phase mode of operation, the fringe pattern is modulated by a piezoelectric transducer (PZT) and detected by a 100 x 100 diode array camera using a dynamic phase measurement technique. Having both the fringe pattern and phase measurement techniques available in one instrument, provides a powerful interferometer system capable of performing wavefront measurements for a wide spectrum of applications.

The phase operation mode of the Mark III Interferometer System is described in detail in Reference 26.

4.3 Relevance of Measurements

The evaluation of most interferograms results in either a peak-to-valley distortion or an rms distortion for either a reflecting surface or transmitting element. For many applications this one parameter characterization is sufficient. For some applications, the maximum slope of the distortion is also a critical parameter. Distortion slopes are usually specified in units of fringes/unit length, e.g. $1/2$ fringe/cm.

Since it is not the purpose of this bulletin to provide a detailed discussion of the significance of the errors manifest in an interference pattern to systems design and performance, the reader is referred to Reference 19 for information on this topic.

5 Glossary of Terms

Distortion: The departure of an actual fringe pattern, wavefront, or surface from some ideal, best-fitting pattern, wavefront, or surface. The concept of distortion used herein should not be confused with the classical third order aberration of the same name.

Fringe: A bright or dark band on an interferogram resulting from the constructive or destructive interference when parts of a divided wavefront are recombined.

Fringe Spacing: The space between fringes of like nature on an interferogram. One fringe spacing corresponds to a one-wavelength optical path difference between the interfering wavefronts. The interpretation of this spacing in terms of the item under test is dependent upon the particular interferometric configuration and the specific test setup. The interferogram scale factor provides this relation.

Interferogram Scale Factor: The quantitative relation defining the correspondence between fringe spacing and the parameter of interest.

Interferometer, Double-Pass Type: An interferometer whose measurement beam traverses the item under test once and is then reflected back through the item under test a second time usually by an auxiliary reflector. The measurement beam thusly traverses the item under test twice. Twyman-Green and Fizeau interferometers are typical examples of double-pass interferometers.

Interferometer, Multiple Beam: An interferometer in which the interference pattern results from the interference of many beams (wavefronts) to produce narrow fringe profiles. The Fizeau interferometer with high reflectivity cavity elements is an example of a multiple beam interferometer.

Interferometer, Single-Pass Type: An interferometer whose measurement beam traverses the item under test only once. The Mach-Zehnder interferometer is an example of a single-pass interferometer.

Interferometer, Two Beam: An interferometer in which the interference pattern results from the interference of only two beams (wavefronts), i.e., the measurement beam and the reference beam to produce broad \cos^2 fringe profiles. Twyman-Green, Fizeau with low reflectivity cavity elements, and Mach-Zehnder interferometers are examples of two-beam interferometers.

Optical Path Length: The product of the geometrical distance traveled by light in a medium and the refractive index of the medium.

Optical Path Difference (OPD): The difference in optical paths of interest. Distortion is an example of one measure of this difference.

Peak-to-Valley Distortion: The algebraic difference between the most positive distortion and the most negative distortion.

RMS Distortion: The root-mean-square value of the distortion. For randomly distributed errors, the rms \approx (peak-to-valley)/4.5.

Wavefront: A surface of constant phase in a light beam.

Zero-Order: The interference fringe which corresponds to zero optical path difference between the interfering wavefronts.

6 References

1. C. A. Zanoni, "Interferometry: the Technology," *The Optical Industry & Systems Directory*, Bk 1, p. B-391
2. D. Malacara, *Optical Shop Testing* (John Wiley & Sons, New York, 1978).
3. A. H. Guenther and D. H. Liebenberg, *Optical Interferograms — Reduction and Interpretation* (American Society for Testing Materials, Philadelphia, 1978).
4. R. A. Jones and P.L. Kadakia, "An Automated Interferogram Technique," *Appl. Opt.*, v. 7, p. 1477 (1968).
5. W. E. Williams, *Applications of Interferometry* (John Wiley and Sons, New York, 1954).
6. C. Candler, *Modern Interferometers* (Hilger & Watts Ltd., London, 1951).
7. M. Francon, *Optical Interferometry* (Academic Press, New York, 1966).
8. G. R. Fowles, *Introduction to Modern Optics* (Holt, Rinehart and Winston, Inc., New York, 1968).
9. L. R. Heintze, H. D. Polster, and J. Vrabel, "A Multiple-Beam Interferometer for Use with Spherical Wavefronts," *Appl. Opt.*, v. 6, p. 1924 (1967).
10. D. J. Herriott, "Multiple-Beam Interference Fringes at Large Plate Spacing," *J. Opt. Soc. Am.*, v. 55, p. 614A (1965).
11. W. H. Steel, *Interferometry* (Cambridge University Press, Cambridge, 1967).
12. J. Strong, *Concepts of Classical Optics* (W. H. Freeman and Co., San Francisco, 1958).
13. E. Wolf and M. Born, *Principles of Optics* (Pergamon Press, New York, 1959).
14. R. Kingslake, "The Interferometer Patterns Due to the Primary Aberrations," *Trans. Opt. Soc.*, London, v. 27, p. 94 (1927).
15. Gallagher, *et al.*, U. S. Patent 3,694,088, September 26, 1972.
16. J. H. Bruning, *et al.*, "Digital Wavefront Measuring Interferometer for Testing Optical Surfaces and Lenses," *App. Opt.*, v. 13, p. 2693 (1974).
17. W. H. Augustyn, Jr., *et al.*, "On-line Scanning of Fringe Data and MTF Computation," *Proc. SPIE*, v. 46, p. 144 (1974).
18. W. H. Augustyn, "Versatility of a Microprocessor-Based Interferometric Data Reduction System," *Proc. SPIE*, v. 192, p. 128 (1979).
19. E. L. O'Neill, *Introduction to Statistical Optics* (Addison Wesley Publishing Co., Reading, MA, 1963).
20. N. Balasubramanian, U.S. Patent 4,225,240 (9/1980).
21. J. C. Wyant, *Appl. Opt.*, vol. 14, p. 2622 (1975).
22. K. D. Stumpf, *Proc. SPIE*, vol. 153, p. 42 (1978).
23. F. M. Mottier, *Proc. SPIE*, vol. 153, p. 133 (1978).
24. N. A. Massie, R. D. Nelson, S. Holly, *Appl. Opt.*, vol. 18, p. 1797 (1979).
25. N. A. Massie, *Appl. Opt.*, vol. 19, p. 154 (1980).
26. M. Schaham, *Proc. SPIE*, vol. 306, p. 183 (1981).
27. J. C. Wyant, *Laser Focus*, vol. 18 (#5), p. 65 (May, 1982).

Acknowledgments

The computer generated interferograms and wavefront contours in Figures 3.2-3, 3.2-4, and A-1 through A-10 were provided by Mr. Ralph McDonough of the Itek Corporation. The computer generated interferograms in Figures A-11 through A-20 were provided by Professor Roland Shack of the Optical Sciences Center of the University of Arizona. Zygo wishes to thank Mr. McDonough and Professor Shack for permission to use their figures in this bulletin.

Appendix A

Interferograms Representing Individual and Combinations of Classical Aberrations

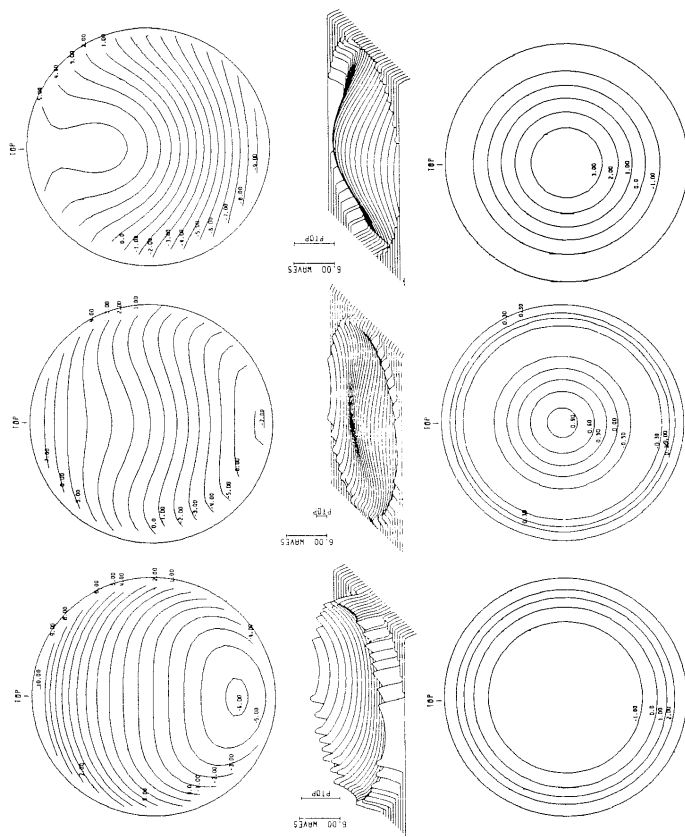


Figure A-1
Spherical Aberration Best Focus

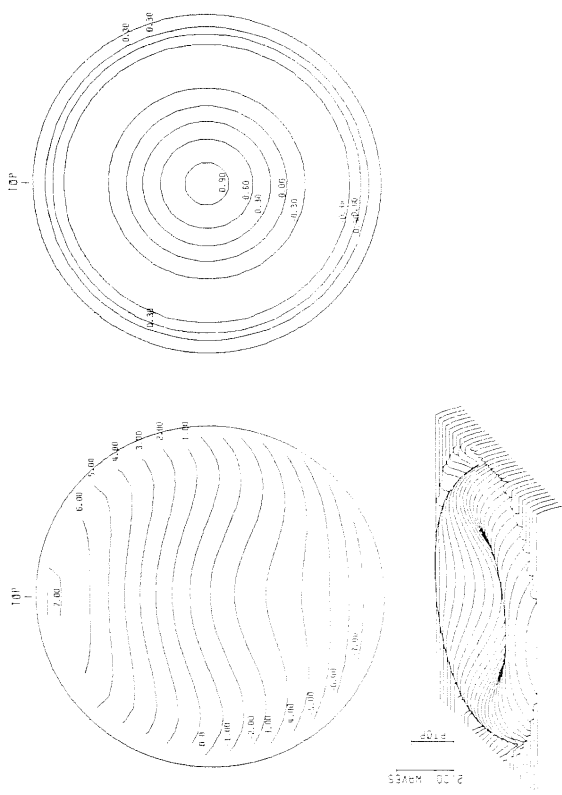


Figure A-2
Spherical Aberration Focusing Effects

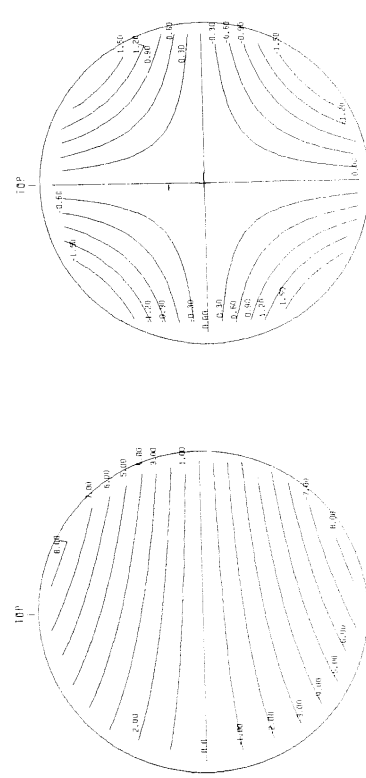


Figure A-3
45-Degree Cylinder Best Focus

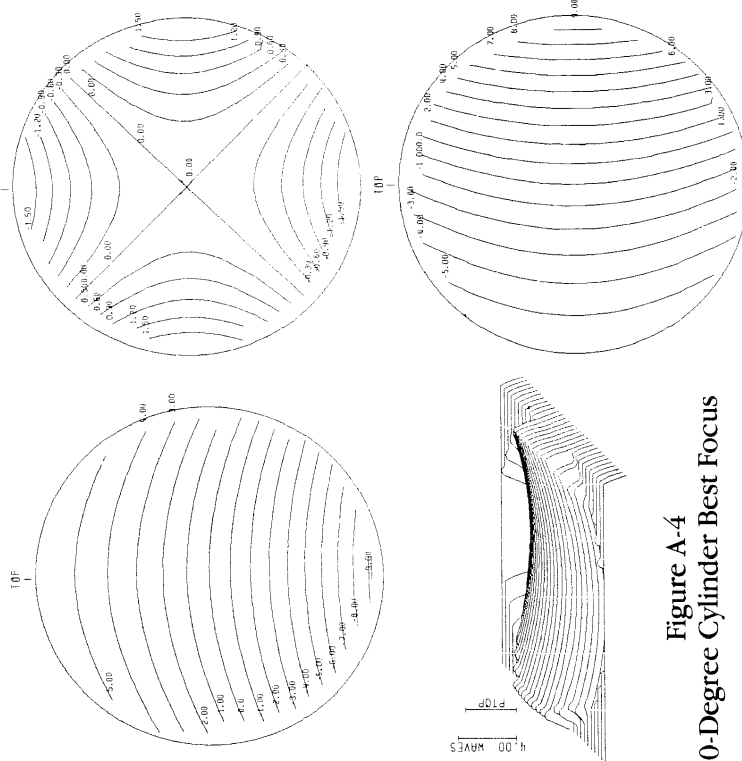


Figure A-4
0-Degree Cylinder Best Focus

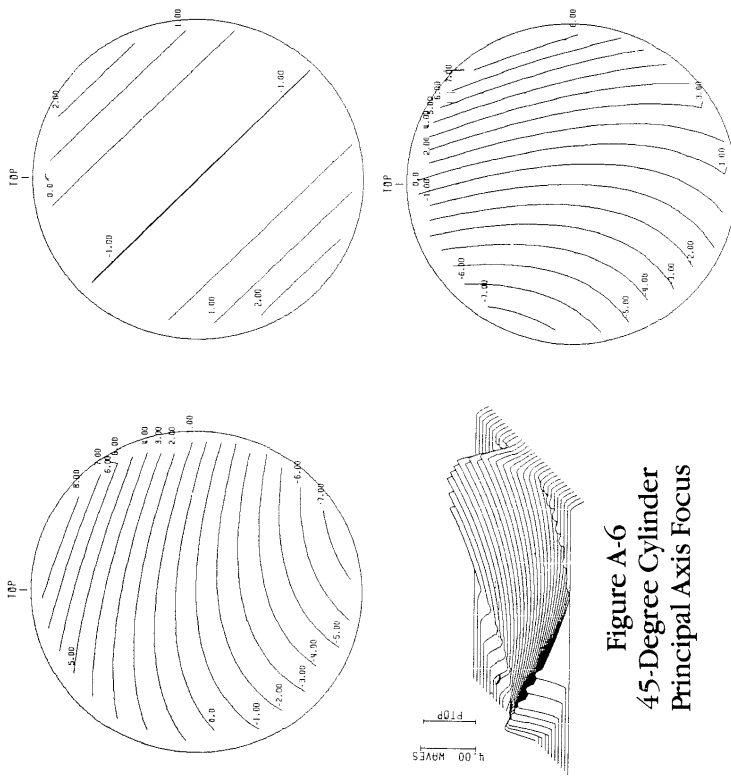


Figure A-5
0-Degree Cylinder
Principal Axis Focus

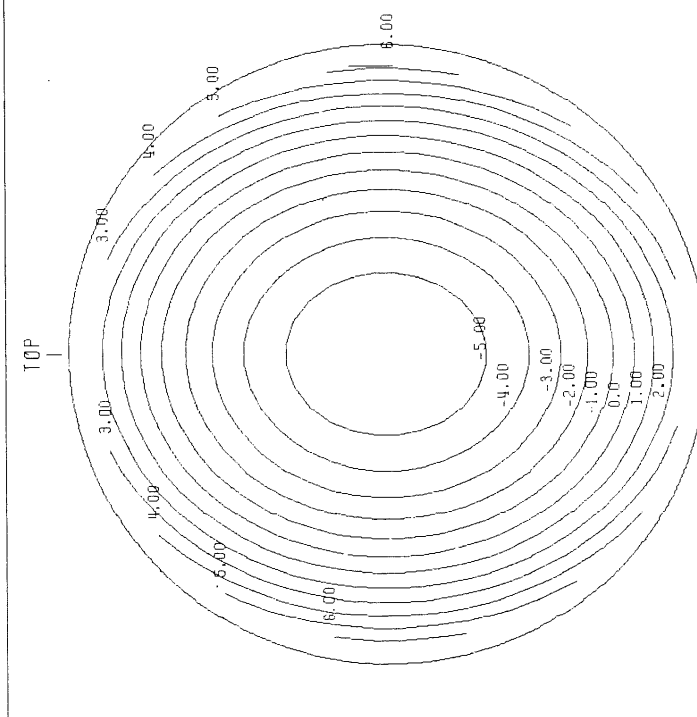


Figure A-7 Bullseye with Cylinder

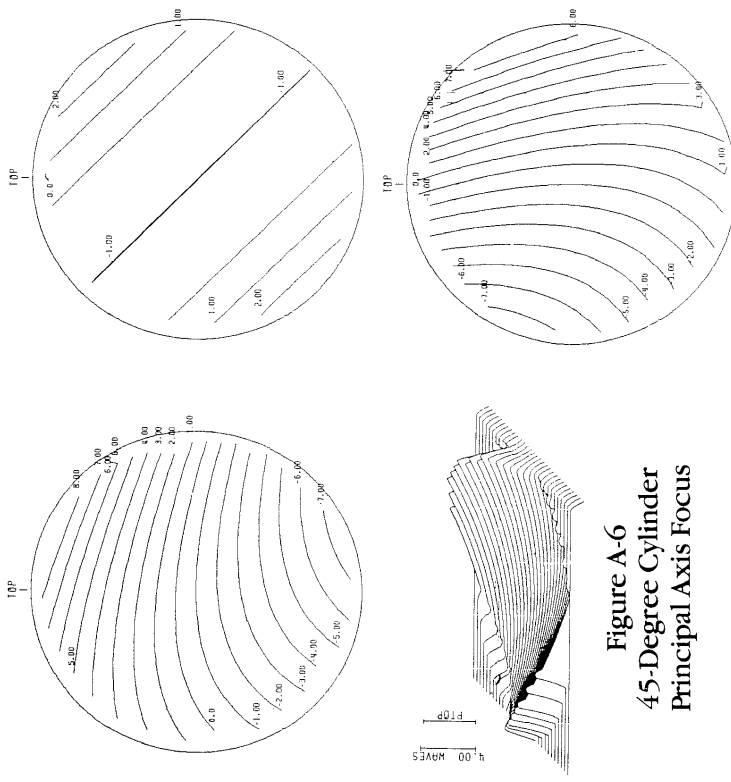


Figure A-6
45-Degree Cylinder
Principal Axis Focus

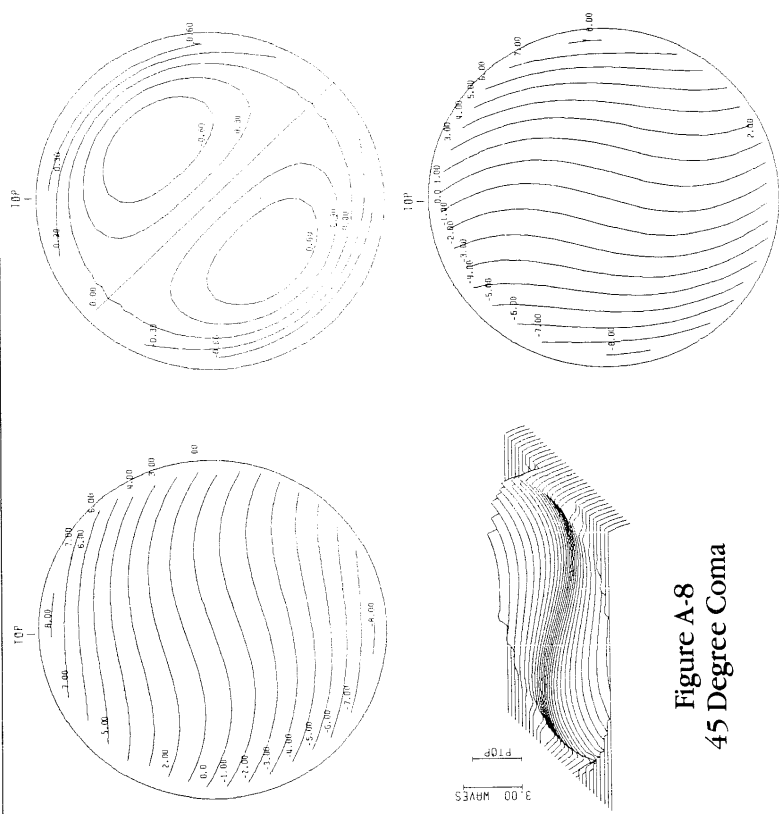


Figure A-8
45 Degree Coma

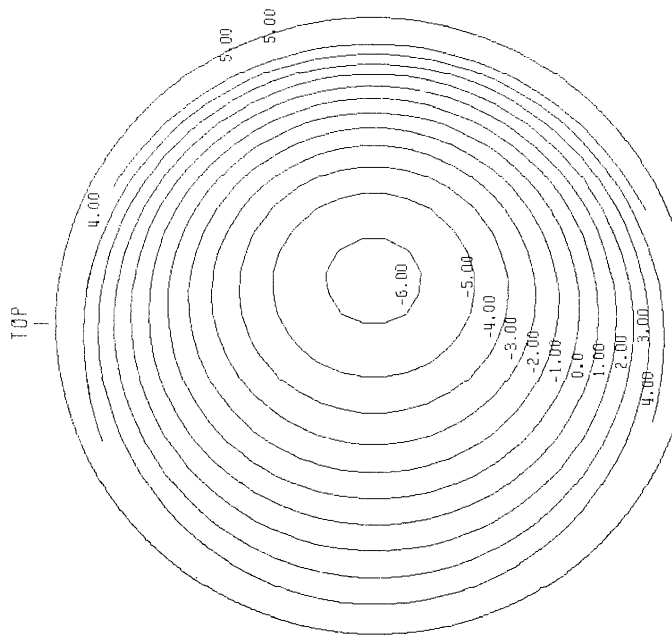


Figure A-10 Bullseye with Coma

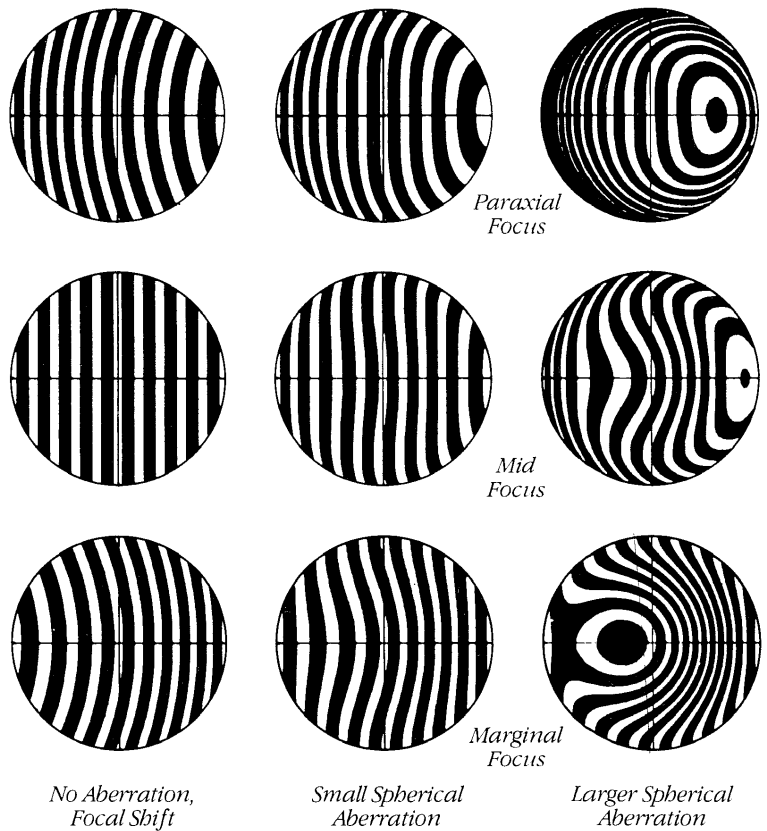


Figure A-11
Interferograms, Spherical Aberration

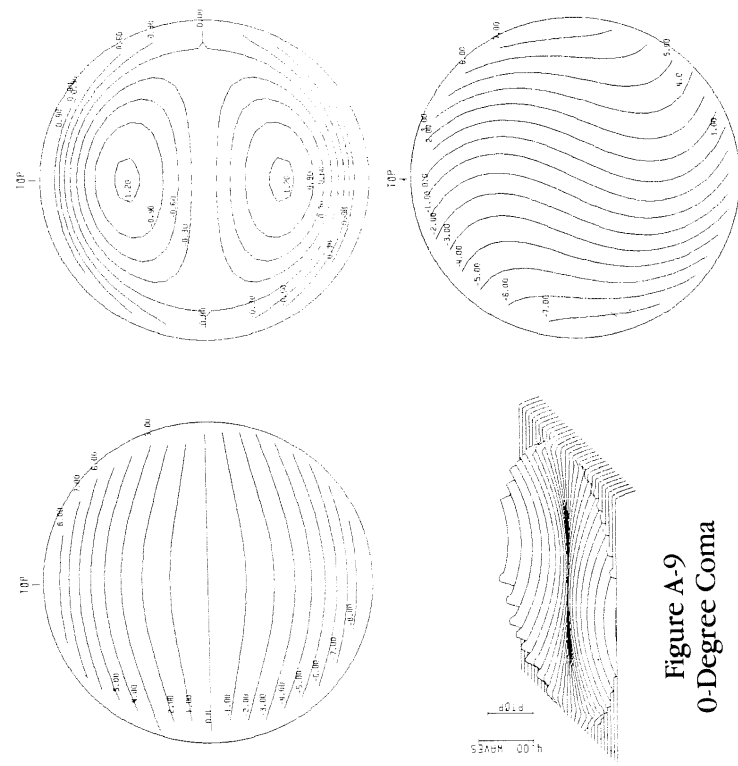


Figure A-9
0-Degree Coma

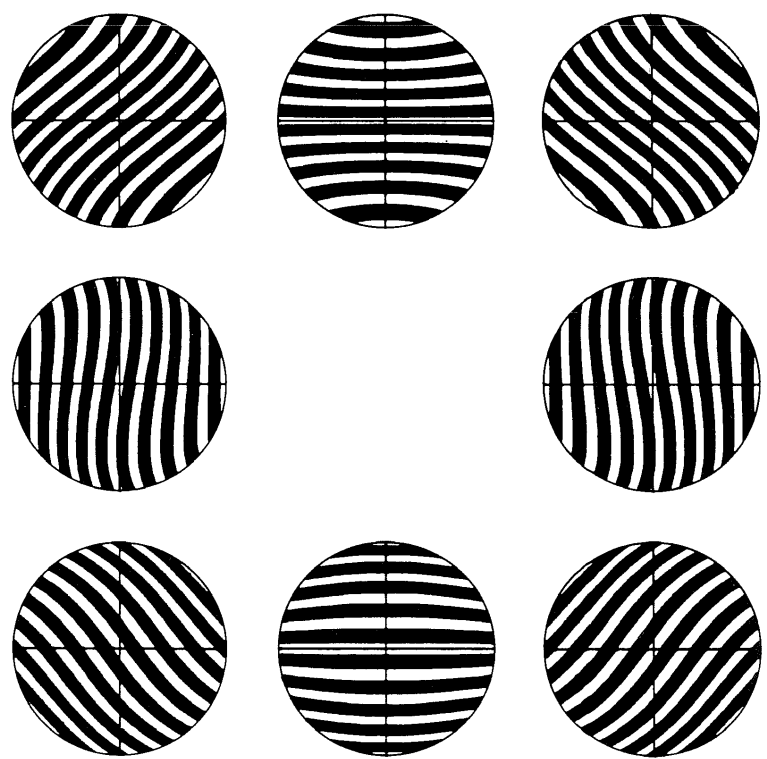


Figure A-12
Interferograms, Small Coma, Large Tilt

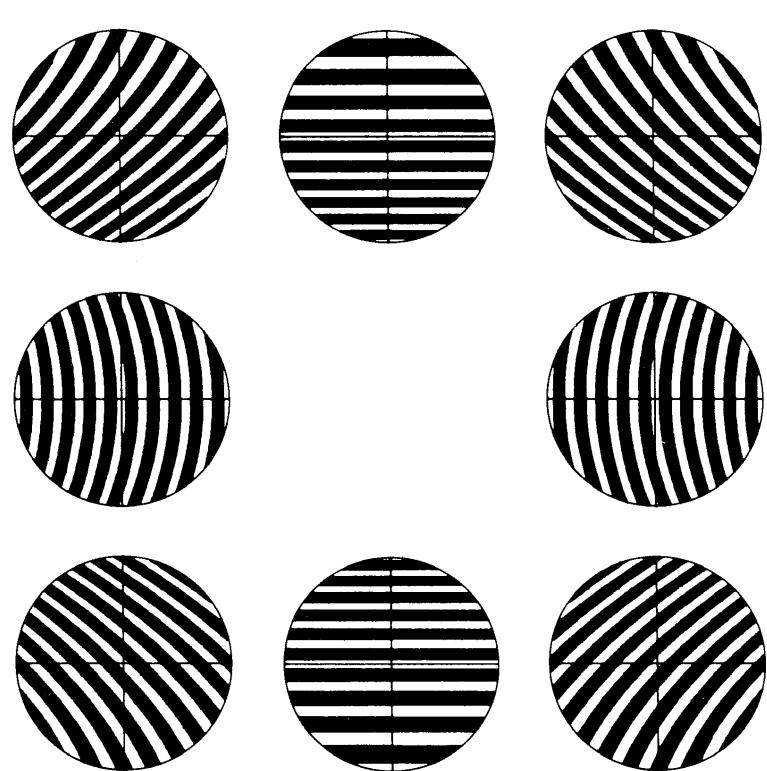


Figure A-13
Interferograms, Small Astigmatism, Sagittal Focus

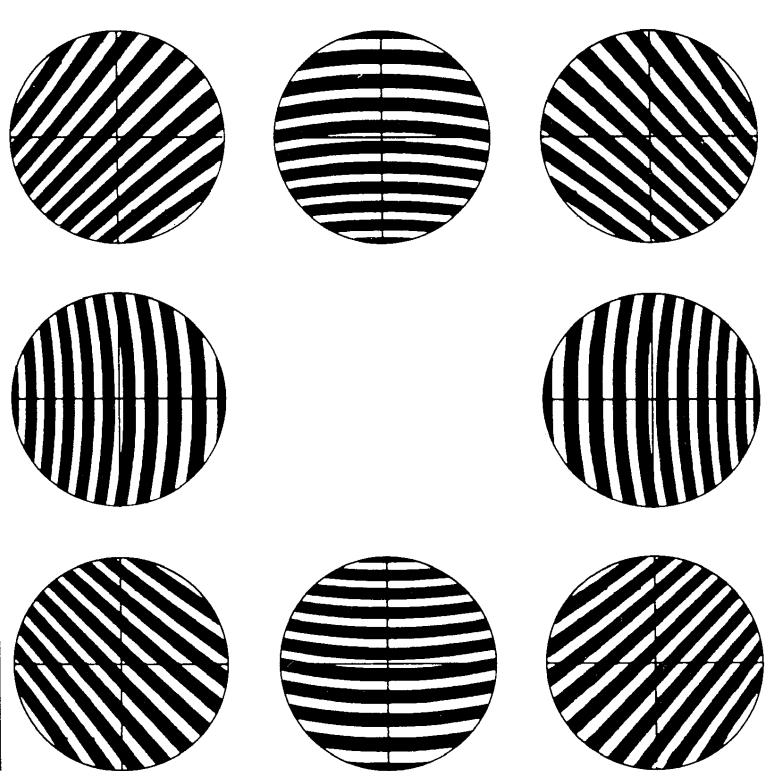


Figure A-14
Interferograms, Small Astigmatism, Medial Focus

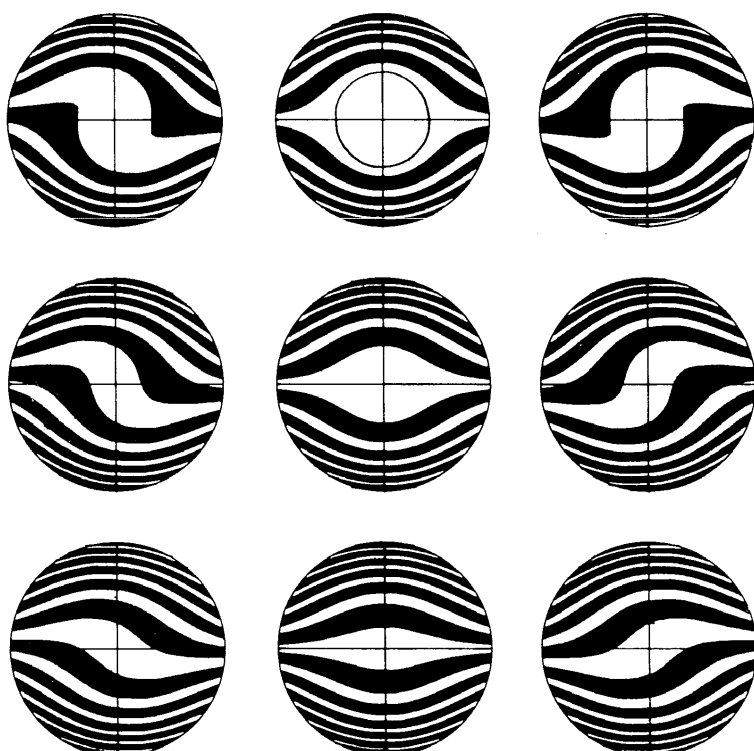


Figure A-15
Interferograms, Large Coma, Large Tilt

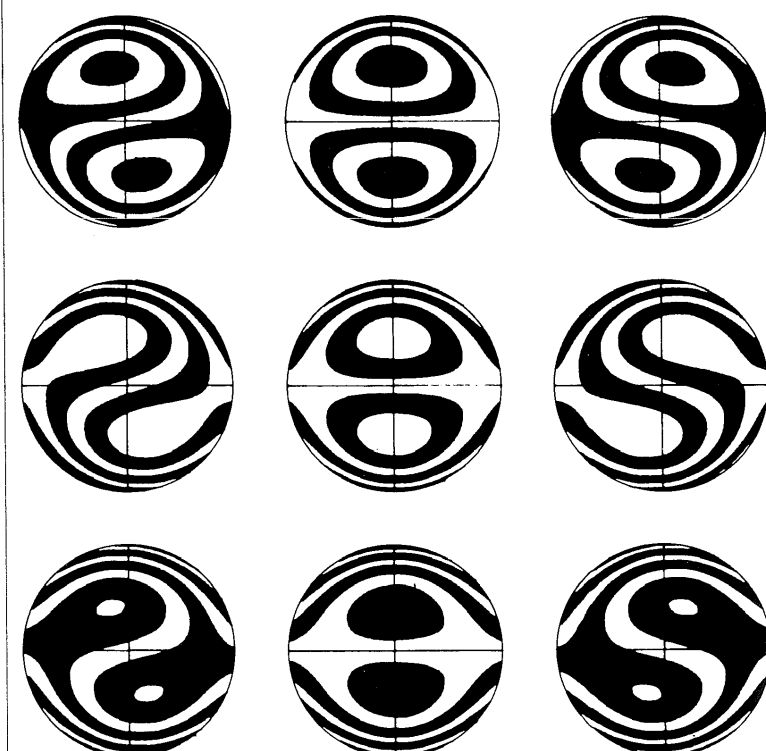


Figure A-16
Interferograms, Large Coma, Small Tilt

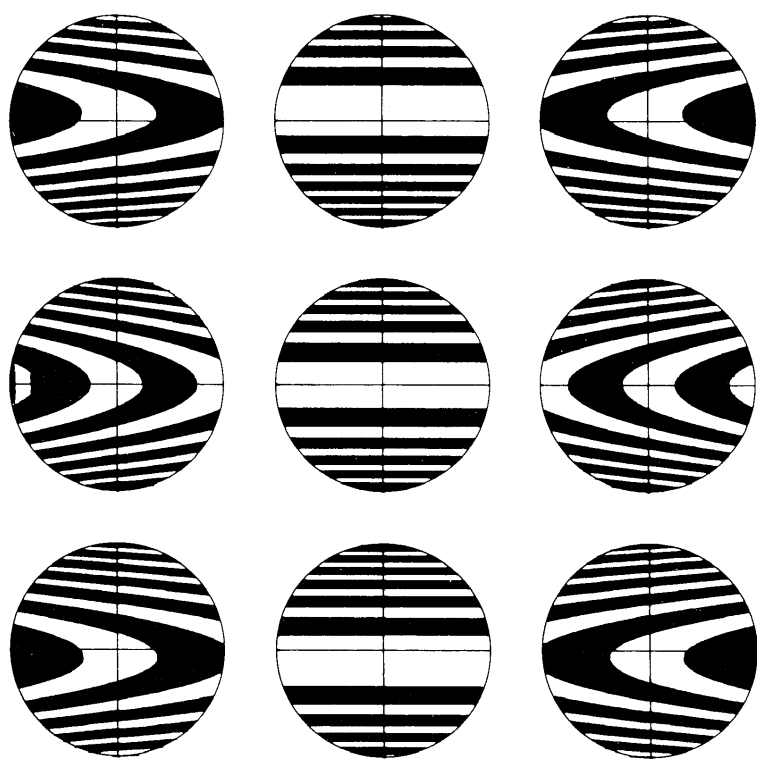


Figure A-17
Interferograms, Large Astigmatism,
Sagittal Focus, Small Tilt

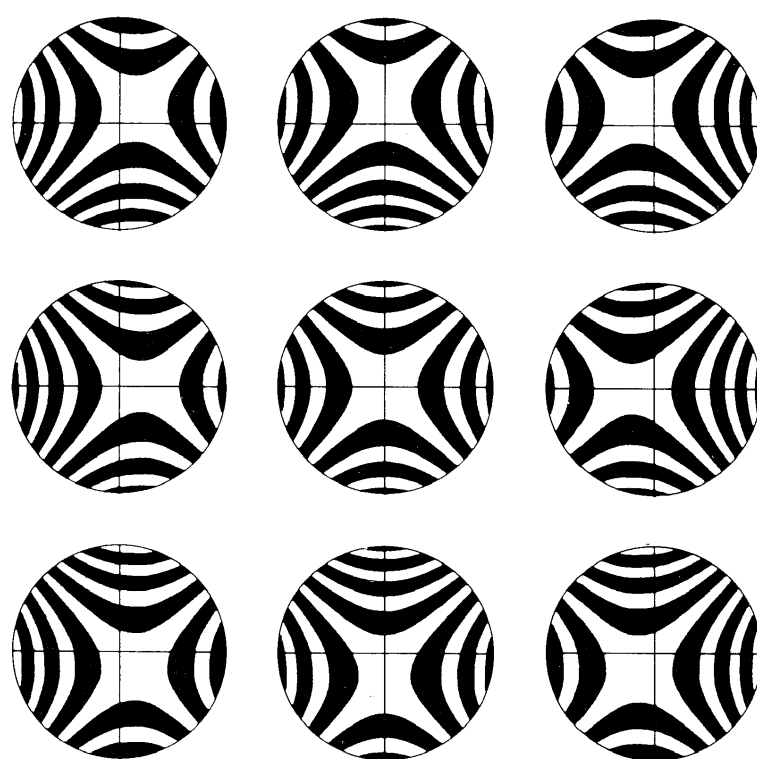


Figure A-18
Interferograms, Large Astigmatism,
Medial Focus, Small Tilt

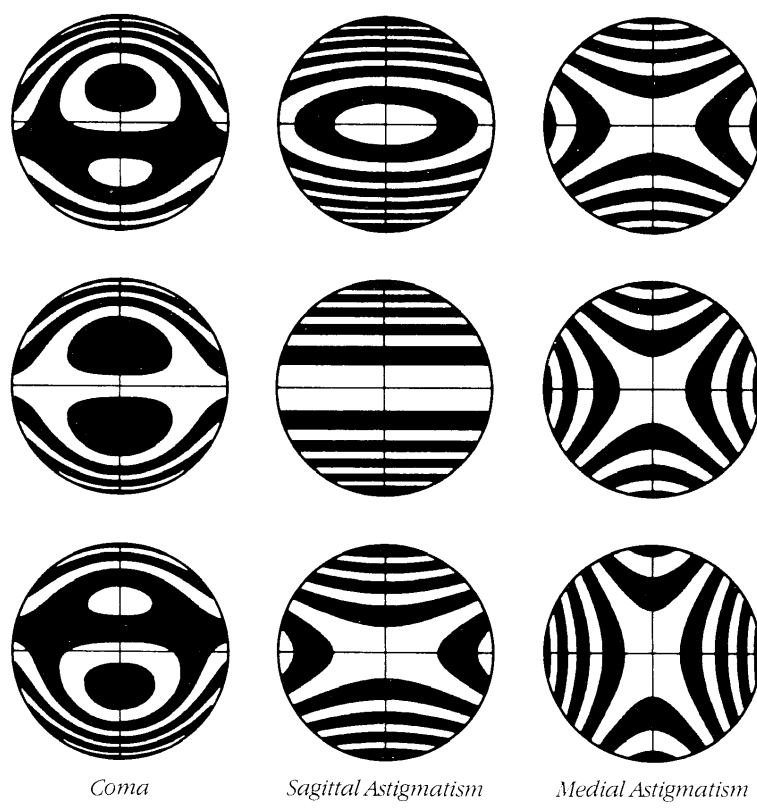


Figure A-19
Interferograms, Small Focal Shift

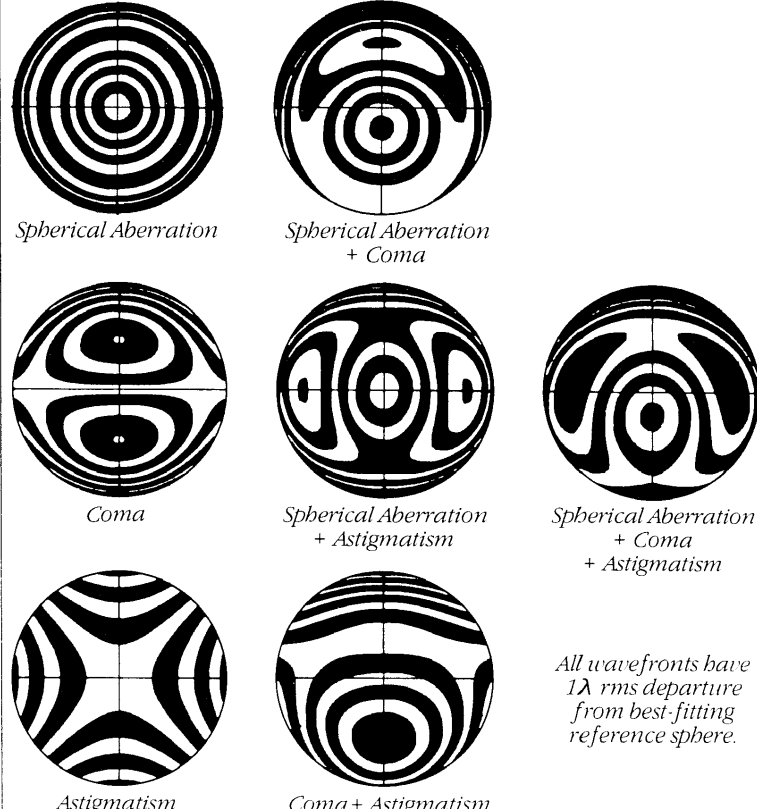


Figure A-20
Interferograms, Combined Aberrations

All wavefronts have
 1λ rms departure
from best-fitting
reference sphere.

Appendix B

Sample Interferograms with Evaluation Results

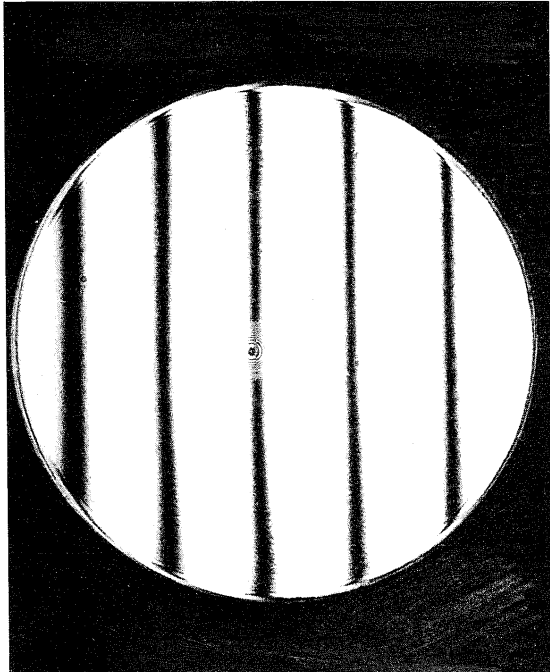


Figure B-1
Peak-to-Valley Distortion = 0.10 Fringe

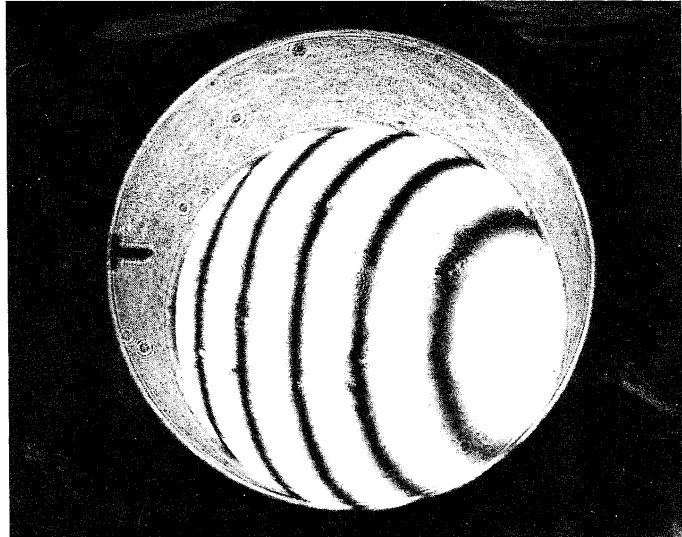


Figure B-2
Peak-to-Valley Distortion = 1.33 Fringe

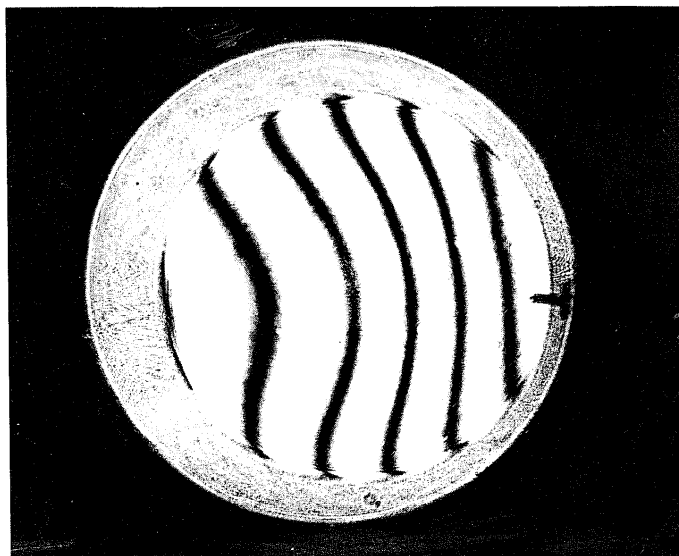


Figure B-3
Peak-to-Valley Distortion = 1.00 Fringe

Epilogue

As you use this booklet, you will come across sections that discuss the merits of "electronic parallelograms" and "automatic pattern processors." And you may be thinking how these devices, and the measurements they provide, seem somewhat out of date in light of the capabilities of Zygo's current products. Well, they are.

Keep in mind that, when earlier editions of this booklet were published, Zygo's ZAPP and FRINGE interferogram analysis systems were remarkable machines, providing their users with powerful automated fringe pattern analysis that was quick, repeatable, and accurate. Although that technology is now obsolete, it was decided that the material should remain in the booklet to provide an historical perspective from which to view the technological advancements that have been achieved since then.

A major step forward came with Zygo's development of the phase measuring interferometer system. Instead of measuring only the spatial locations of the fringe centers, as with our previous systems, this system measures phase differences between various points in the aperture while the cavity length is precisely modulated. The main benefits of this system are a tremendous increase in measurement accuracy and the ability to analyze complex interference patterns.

The other significant event that led to the current level of interferometric measurement came about more gradually; however, if we make a "then-vs.-now" comparison, the progress has been astounding. The reference is to the "computer revolution," the exponential increase in affordable computing power that took off in the 1980's, and continues today.

The fringe analysis functions of Zygo's interferometer systems used to be performed on a proprietary computer system designed and manufactured by Zygo. The in-house computer design was necessary because existing computer systems with sufficient processing power were prohibitively expensive. The custom system performed very well; however, as off-the-shelf computers became more powerful and less expensive, it became practical to use them in

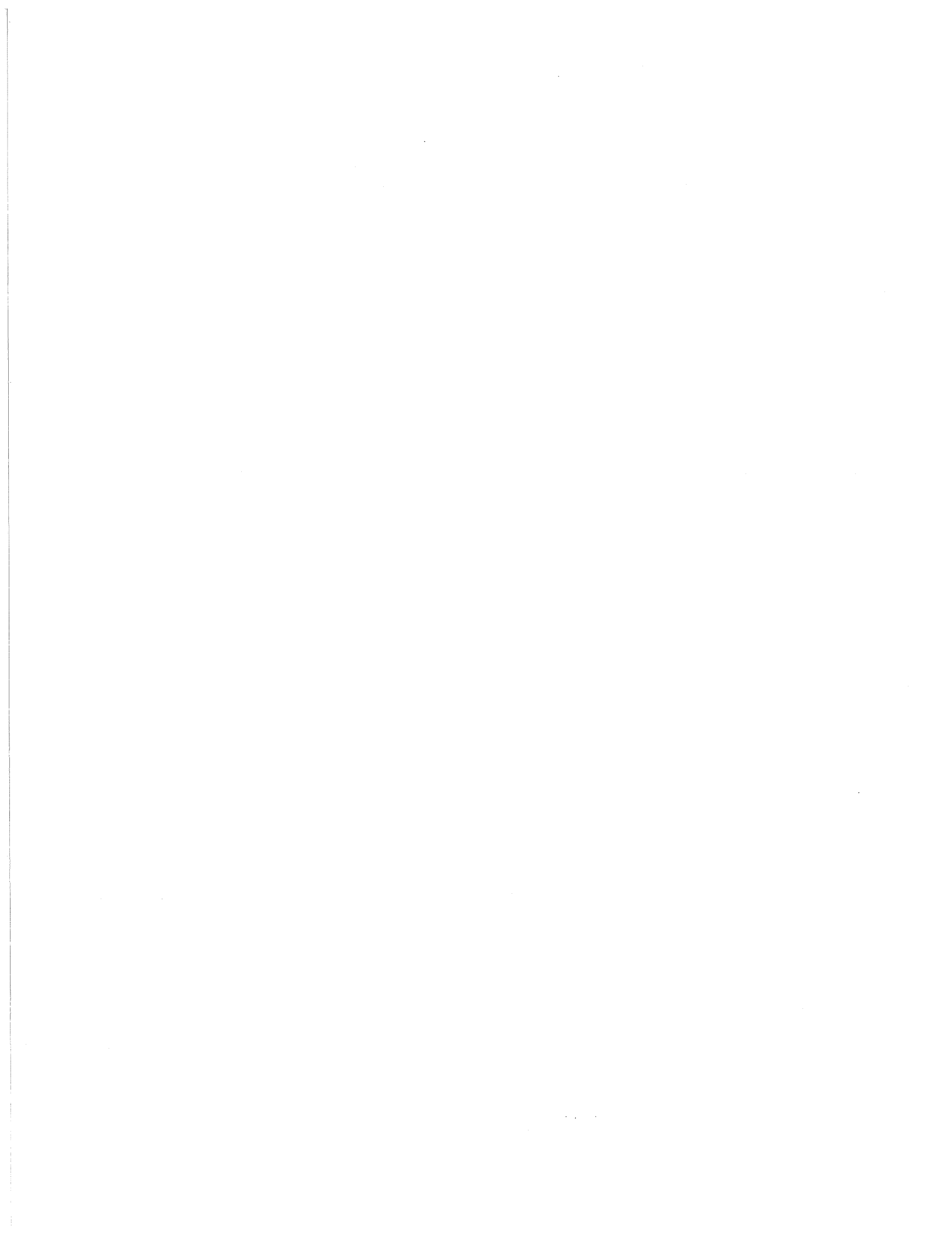
the interferometer systems. This change allowed Zygo's technical resources to focus on creating data analysis software that would take full advantage of the computing power that had become available.

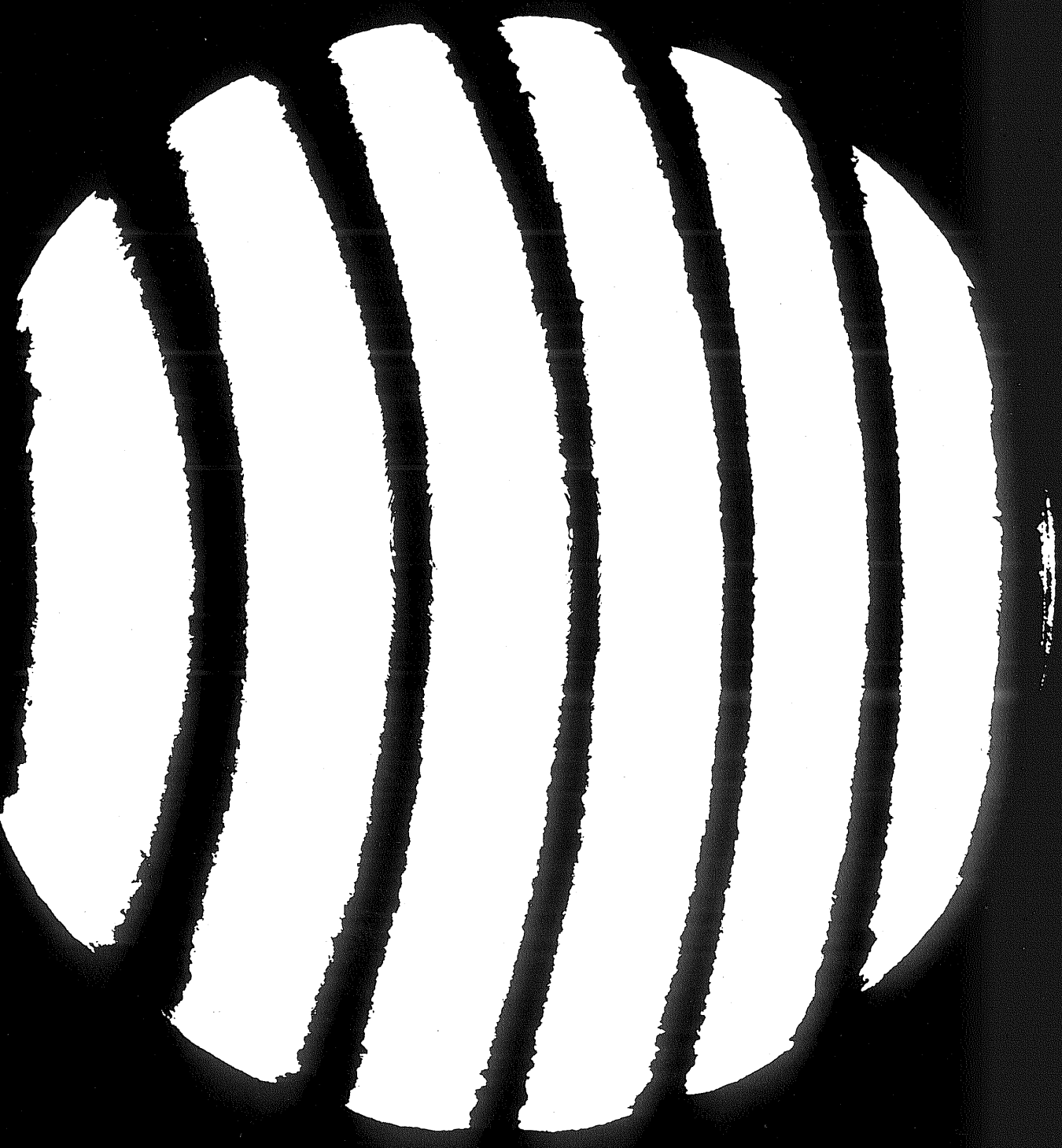
Whereas measurement results and surface plotting were fairly basic in the past, providing peak-to-valley, rms, and power values, and a coarse surface plot, the latest MetroPro™ software also provides gradients, Zernike polynomials, third-order aberrations, PSF, MTF, and a variety of statistical process control capabilities. Information can still be provided numerically, but it is also represented with high-resolution, 3-dimensional, rotatable color plots and sliced cross sections. All of this complex processing now takes just a few seconds.

The benefactors of all these technological improvements are our customers. Greater accuracy and more flexible analysis capabilities provide optical manufacturers with the tools required to refine their fabrication and polishing processes. Surfaces are routinely qualified to 1/100th wave, peak-to-valley; prism angles are measured to 0.1 arc second; and material index homogeneity is measured to better than 1×10^{-6} . This level of measurement precision is required for the manufacture of today's most critical components, such as the microlithography equipment used in semiconductor manufacturing and the components used in high-power laser fusion research.

Just as today's data analysis capabilities are far and away better than those of the past, tomorrow's technologies promise to bring even greater capabilities at a lower cost. The only thing that will not change is Zygo's commitment to develop and apply new technologies to the field of precision measurement, providing our customers with the finest instruments available.

If you would like to learn more about Zygo's interferometric measuring instruments, or if you think you have an application that could benefit from the resolution and accuracy of interferometry, please contact a Zygo Applications Engineer at (203) 347-8506, or Fax (203) 347-8372.





zygo

Zygo Corporation
Laurel Brook Road
P.O. Box 448
Middlefield, CT 06455-0448
U.S.A.

Headquarters: (203) 347-8506
Fax: (203) 347-8372

Rochester, NY: (716) 586-3560
Santa Clara, CA: (408) 982-1155

AB-0001A 4/93 3M

Copyright © 1977 Zygo Corporation
Printed in the U.S.A.

zygo® is a registered trademark of
Zygo Corporation